Chapter 5
The Salivary Glands

Ricardo H. Bardales

Normal Salivary Glands

The three pairs of major salivary glands include the parotid, submandibular, and sublingual. The minor salivary glands are numerous and are located in the mouth and oropharynx.

All salivary glands are exocrine and have serous or mucous acini and excretory ducts. Serous acini have basally located nuclei, granular basophilic cytoplasm, and cytoplasmic zymogen PAS+ diastase-resistant granules, and they secrete amylase (Fig. 5.1). Mucous acini have basally located nuclei, clear vacuolated cytoplasm, and cytoplasmic sialomucin vacuoles, and they secrete mucin. The ductal system begins distally in the intercalated ducts, which are lined with cuboidal epithelium. The cells have central nuclei in communication with the larger striated ducts which are lined by mitochondria-rich columnar eosinophilic cells. The more proximal interlobular ducts are lined by pseudostratified columnar epithelium with scattered mucinous cells. Myoepithelial cells surround the secretory acini and the intercalated ducts.

R.H. Bardales, MD, MIAC, ECNU
Department of Pathology and Cytopathology,
Outpatient Pathology Associates,
7750 College Town Drive, Sacramento, CA 95826, USA
e-mail: rhbardales@aol.com

R.H. Bardales (ed.), *The Invasive Cytopathologist*, Essentials in Cytopathology 16, DOI 10.1007/978-1-4939-0730-4_5,

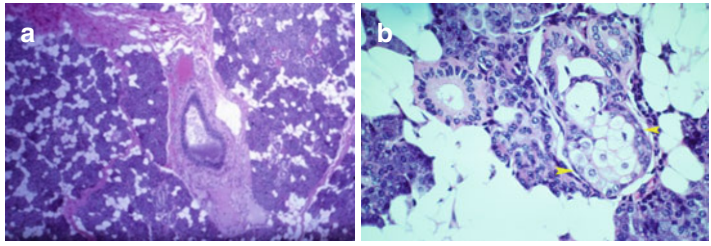

FIGURE 5.1 Normal histology of the parotid gland at low (**a**) and high magnification (**b**). Note the presence of adipose tissue and sebaceous glands (**b**, *arrowheads*) (Hematoxylin and eosin stain)

The parotid gland is a serous gland and contains lymphoid aggregates; lymph nodes may be present and contain ducts or occasionally acini. The submandibular gland is mixed serous and mucous; caps of serous cells may be seen in the mucous acini. The sublingual gland is also mixed but is predominantly mucous. The minor glands may be predominantly serous or mucous.

Ultrasound of the Salivary Glands

The parotid space extends from the external auditory canal superiorly to the angle of the mandible inferiorly, neighbors the nasopharyngeal area in the medial aspect, and is separated from the carotid space by the posterior belly of the digastric muscle. The space contains the parotid gland, facial nerve, retromandibular vein, external carotid area, and lymph nodes. The normal parotid gland has a homogeneous echotexture and is hyperechoic, more than the submandibular gland (Fig. 5.2). The facial nerve cannot be visualized; however, the retromandibular vein, seen as a well-defined hypoechoic tubular structure, is the landmark for the facial nerve. Intraparotid lymph nodes may be visualized, measure <5 mm, and are usually located in the superficial lobe. An accessory parotid gland may be seen in 20 % of patients and is located overlying the masseter muscle.

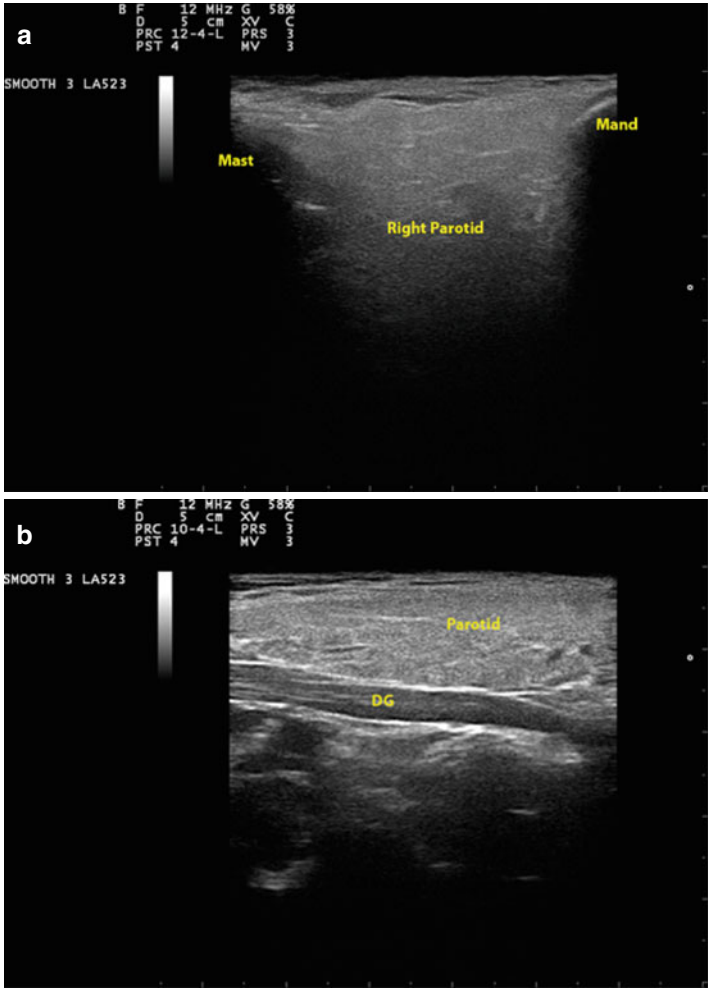

FIGURE 5.2 Normal US of the parotid space and parotid gland (**a**, right parotid; **b**, left parotid). *Mand* mandible, *Mast* mastoid process, *DG* posterior belly digastric muscle

The submandibular and sublingual spaces lay inferolateral and superomedial, respectively, and are divided by the mylohyoid muscle. The submandibular space contains

the anterior belly of the digastric muscle, the superficial lobe of the submandibular gland, lymph nodes, the facial artery and vein, the inferior part of the XII nerve, and fat. Different from the parotid gland, the lymph nodes are around and not within the submandibular gland. The sublingual space contains the anterior hyoglossus muscle, the deep lobe of the submandibular gland, sublingual gland and ducts, submandibular duct, lingual artery and vein, lingual nerve, and cranial nerves IX and XII. The submandibular and sublingual glands are homogeneous and slightly hyperechoic. The Wharton's duct is not normally seen, only when dilated (Fig. 5.3).

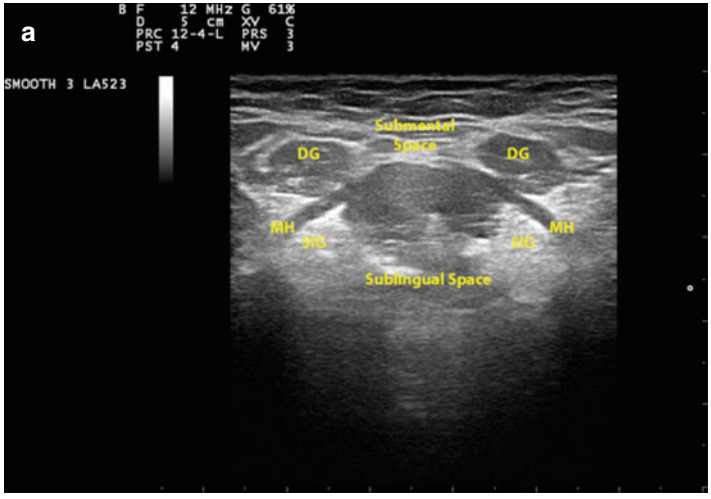

FIGURE 5.3 Normal US of the submental and sublingual (**a**, transverse view; **b**, longitudinal view), and submandibular (**c**) gland spaces and the submandibular gland. *DG* digastric muscle, *MH* mylohyoid muscle, *SlG* sublingual gland, *LN* lymph node, *SmG* submandibular gland, *DGa* anterior belly digastric muscle, *DGp* posterior belly digastric muscle, *HG* hyoglossus muscle, *T* tonsil

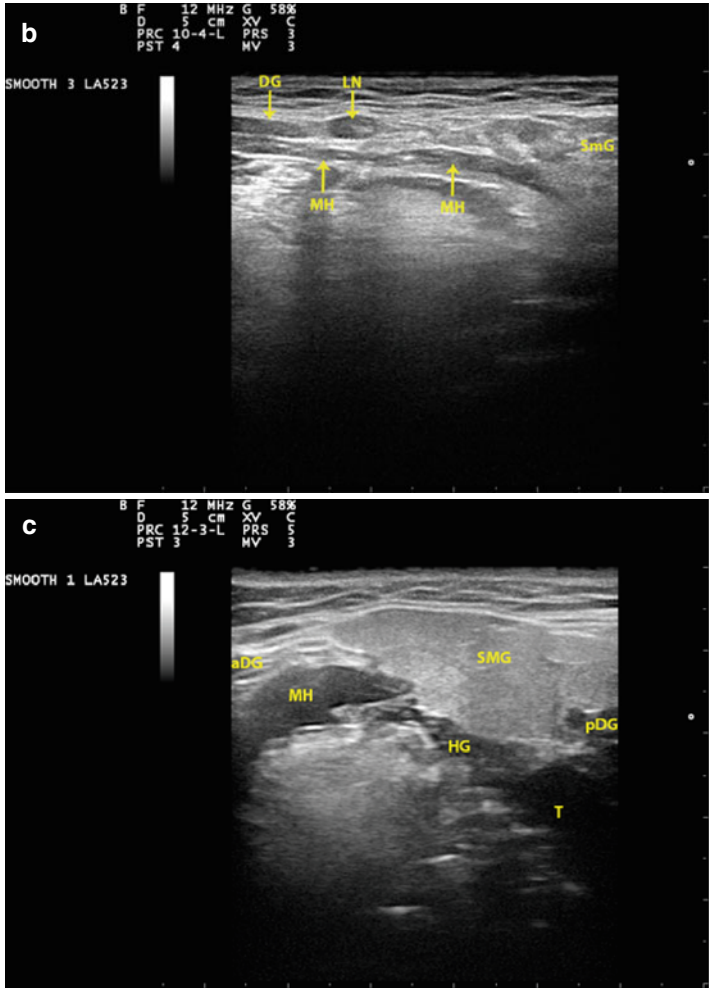

FIGURE 5.3 (continued)

US and Salivary Gland Masses

US imaging alone is usually sufficient for evaluation of most salivary gland masses. However, US has limitations: it cannot visualize the deep lobe of the parotid gland and the minor

salivary glands. Thus, masses arising deep in the parotid gland, oral cavity, tracheobronchial tree, or pharynx cannot be evaluated by US. In cases of salivary gland malignancies, US cannot evaluate bone, perineural, or deep-soft-tissue involvement or the retropharyngeal lymph nodes. Despite these limitations, US should be part of the initial evaluation of any accessible asymptomatic salivary gland mass, particularly when it develops in the parotid, submandibular, or sublingual areas. Of note, 20 % of masses clinically considered as being in the parotid gland are extra-glandular and reinforce the use of US. US characterizes a salivary gland mass, evaluates associated lymphadenopathy, and permits needle guidance and accurate sampling by fine-needle aspiration (USG-FNA). USG-FNA is the preferred diagnostic modality for any symptomatic or asymptomatic salivary gland mass.

US Features of Benign and Malignant Salivary Gland Masses

1. *Tumor edge*. Benign tumors have well-defined, regular, and smooth margins. Malignant tumors have irregular and ill-defined contours (Fig. 5.4).
2. *Internal architecture*. Benign tumors have a homogeneous echotexture and may have posterior acoustic enhancement as often seen in pleomorphic adenomas. Malignant tumors have heterogeneous internal architecture and may have areas of necrosis and cystic change/hemorrhage. However, benign tumors may have cystic change and complex internal architecture, i.e., Warthin's tumors or large pleomorphic adenomas. Calcification usually indicates a long-standing process, as seen in pleomorphic adenoma (Fig. 5.5).
3. *Tumor extent*. Extracapsular invasion into the surrounding tissue, including the skeletal muscle, subcutaneous tissue, and skin, may be seen, particularly in high-grade or long-standing malignant tumors (Fig. 5.6).

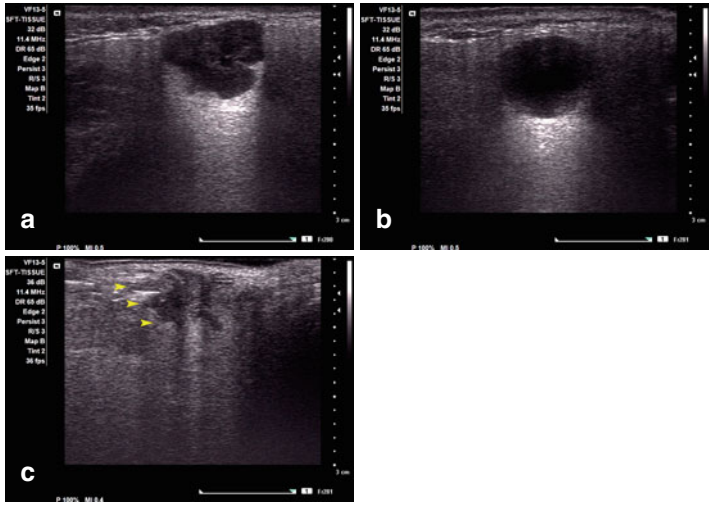

FIGURE 5.4 Tumor edge. Smooth, well-defined, and lobulated borders are often seen in benign mixed tumors or pleomorphic adenomas (**a**). Round and well-defined edges are seen in cystic lesions (**b**). Spiculated infiltrative borders (*arrow heads*) are seen in malignant tumors (**c** adenoid cystic carcinoma)

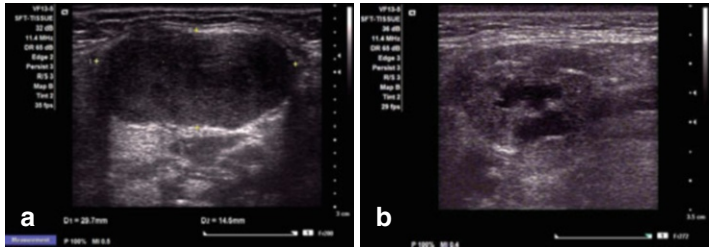

FIGURE 5.5 Internal architecture. Homogeneous echotexture is commonly seen in monomorphic and pleomorphic adenomas (**a** monomorphic adenoma). Heterogeneous echotexture may be seen in malignant tumors (**b** mucoepidermoid carcinoma), chronic sialadenitis (**c**), and benign tumors (**d** Warthin's tumor)

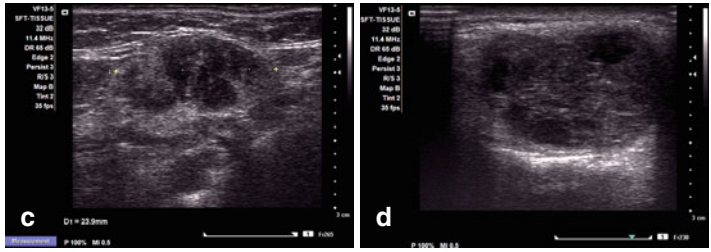

FIGURE 5.5 (continued)

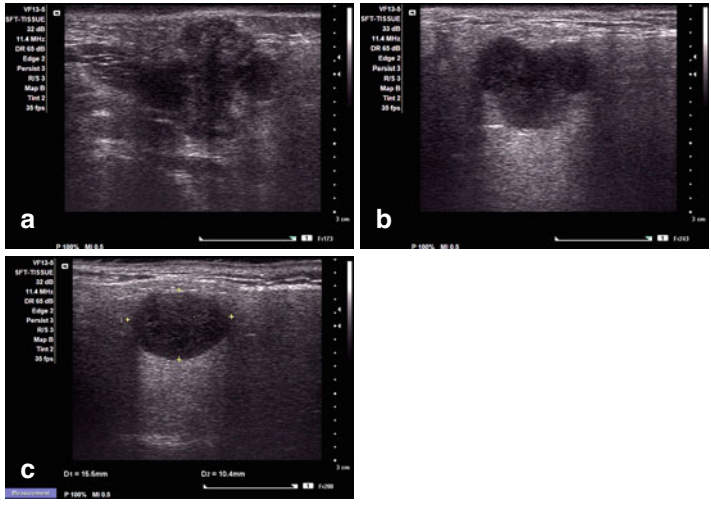

FIGURE 5.6 Tumor extent. Malignant tumors show spiculated and fuzzy borders with infiltration into surrounding tissue (**a** basal cell carcinoma). Smooth and distinct borders are seen in benign conditions (**b** monomorphic adenoma; **c** Warthin's tumor)

4. *Tumor vascularity*. Malignant tumors may show increased internal vascularity. Pleomorphic adenomas may have peripheral vascularity (Fig. 5.7).
5. *Lymphadenopathy*. An indirect sign of malignancy is the presence of cervical lymph nodes with abnormal US features in the region of lymphatic drainage.

The US distinction between benign and malignant salivary gland masses is not clear, and features overlap. Although US imaging is unable to differentiate among specific types of malignant salivary gland tumors, it helps to separate benign from malignant tumors. However, low-grade malignancies often share similar US features with benign tumors.

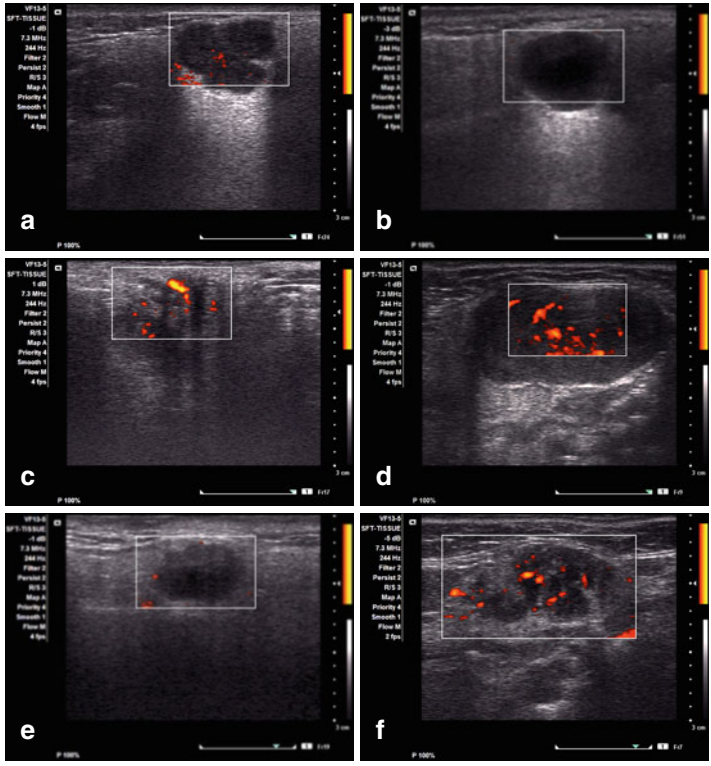

FIGURE 5.7 Tumor vascularity. Vascularity is variable and usually high in high-grade tumors. However, Warthin's tumors usually have high internal vascularity. The tumors shown correspond to those benign and malignant tumors and lesions listed in 4A–C (**a**, pleomorphic adenoma; **b**, cyst; **c**, adenoid cystic carcinoma), 5A–D (**d**, monomorphic adenoma; **e**, mucoepidermoid carcinoma; **f**, chronic sialadenitis; **g**, Warthin's tumor), and 6A–C (**h**, basal cell carcinoma; **i**, monomorphic adenoma; **j**, Warthin's tumor)

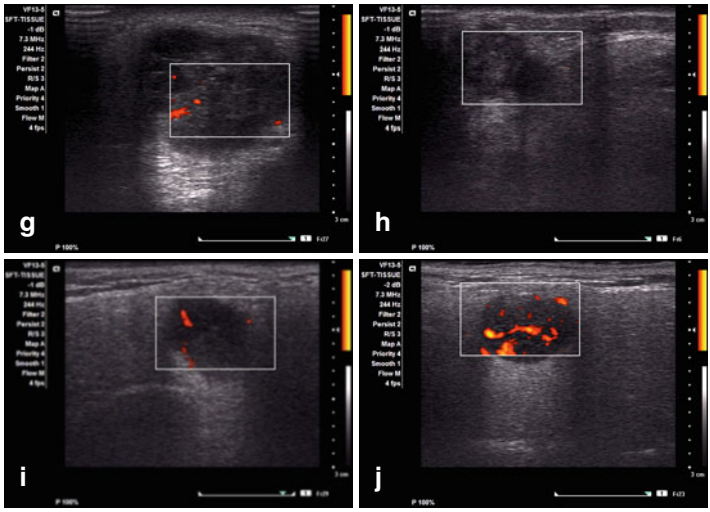

FIGURE 5.7 (continued)

Ultrasound-Guided FNA of Salivary Gland Masses

From the clinical perspective, it is relevant to remember that masses often develop in the parotid, submandibular, sublingual, and minor salivary glands in decreasing order. They may be present in heterotopic salivary gland tissue in various sites of the head and neck, including along Stensen's duct, and most are malignant, with mucoepidermoid carcinoma being the most common. Patient age is relevant because benign mixed tumor and Warthin's tumor occur in adulthood, and mucoepidermoid carcinoma is the most common salivary gland tumor in children. Local pain, facial nerve damage, and signs of local tumor invasion often indicate malignancy, but their absence does not exclude such a diagnosis.

Masses affecting the salivary glands may be broadly classified as infectious/inflammatory, nonneoplastic, and neoplastic with a vast resulting number of mass lesions. Superimposed alterations such as degeneration, chronic inflammation, cystic

change, or metaplasia of various types add challenges to the already at times difficult pathologic diagnosis.

We agree with Stanley, M. W. et al. that a practical approach to interpreting FNA material based on a pattern diagnosis recognition based on first impression key findings will result in a narrow differential diagnosis for that particular pattern. We will adopt this approach to discuss common salivary gland masses. Briefly, the salivary gland patterns include (1) normal, (2) inflammatory/infectious, (3) pleomorphic adenoma, (4) Warthin's tumor, (5) cystic, (6) small epithelial cells, (7) large epithelial cells, and (8) spindle cells. Benign mixed tumor and Warthin's tumor are included not only because they are common but also for their occasional diagnostic difficulties in differentiating them from other tumors. The most common salivary gland masses will be covered in this fashion, and the rare entities will be mentioned briefly.

The USG-FNA is performed with a 25-gauge needle without suction (Zajdela technique), as mentioned in the aspiration procedure section, early in this book. If the material obtained is limited, the use of an aspiration device may be indicated for applying moderate suction (3–4 ml of negative pressure). USG-FNA with a 22-gauge needle may be used for obtaining a bloody specimen, which is useful for preparation of a cell block for histologic evaluation and for ancillary tests including molecular studies; salivary gland tumors have significant and highly prevalent translocations. USG-FNA has 85, 96, and 94 % sensitivity, specificity, and accuracy, respectively, in the evaluation of salivary gland masses. USG-core biopsy may be considered in rare selected cases, solely when USG-FNA is nondiagnostic and the patient's risk for surgery is high.

Pattern I: Normal Salivary Gland Pattern

This pattern may be present in up to 20 % of salivary gland FNAs in some series. Cytologic smears are cellular and show predominantly acinar and less common ductal elements as well as variable amounts of adipose tissue. Acinar elements are arranged in small, round aggregates of cells with large

granulovacuolar cytoplasm, eccentric round nuclei, and small inconspicuous nucleoli. Acinar cells have a fragile cytoplasm; as a result, the smear background is granular and exhibits variable numbers of stripped nuclei that need to be distinguished from lymphocytes, which have a scant rim of basophilic cytoplasm. The ductal elements may be branching and show tubular structures and cell sheets with honeycomb architecture (Fig. 5.8a, b).

Sialosis

Sialosis is a nonneoplastic, asymptomatic salivary gland enlargement that affects principally the parotid gland and less commonly the submandibular gland. It is the result of

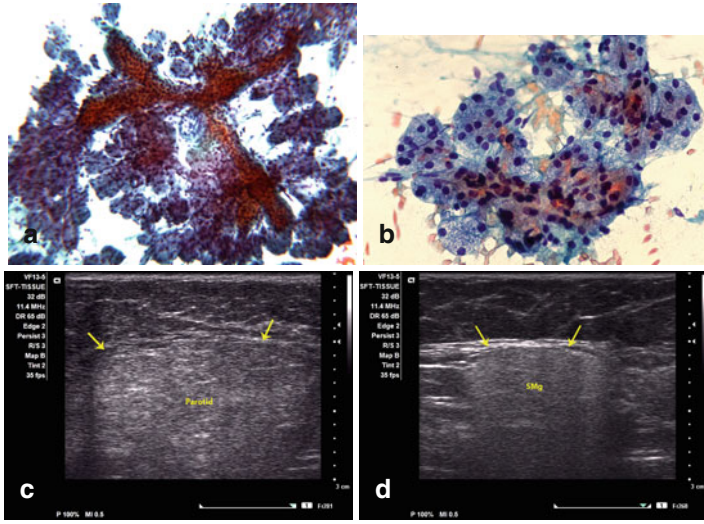

FIGURE 5.8 Normal salivary gland cytology showing cohesive branching ducts and acini (**a**, **b**). US imaging of the left parotid (**c**, *arrows*) and left submandibular (**d**, *arrows*) gland enlargement (sialosis) in a patient with type II diabetes mellitus shows both glands with diffuse homogeneous echotexture and no hyper- or hypoechoic masses. There is a slight hyperechogenicity in the parotid gland compared with the submandibular gland (**c**, **d**) (**a**, **b** Papanicolaou stain, low and high magnification) *SMg* submandibular gland

acinar hypertrophy and is usually bilateral. A related underlying cause is usually identified, i.e., diabetes mellitus, malnutrition, alcoholism, cirrhosis, obesity, hypothyroidism, HIV, drugs, etc.; however, it may be idiopathic. FNA smears show a normal salivary gland pattern, as mentioned before (Fig. 5.8a, b). It has been suggested that the cellular yield is greater than that of normal gland, and acinar cells are 20 % larger than normal cells, features that are difficult to evaluate in a high-quality FNA smear. The aspirates may contain variable amounts of adipose tissue, but they are devoid of inflammatory cells. The differential diagnosis includes failure to sample the target, and depending on the amount of adipose tissue present, a lipoma or a lipomatous salivary gland should be considered, all of which require clinical correlation, including imaging studies. The diagnostic accuracy is improved when the cytopathologist performs USG-FNA to reduce the sampling error.

US features. There is bilateral gland enlargement with normal echogenicity and no focal lesions or increased blood flow; however, the glands may be hyperechoic due to fat infiltration. The features are nonspecific (Fig. 5.8c, d).

Pattern II: Inflammatory/Infectious Pattern and Similar Processes

Acute Inflammation

Acute inflammatory processes most commonly affect the parotid gland but are rarely subject to FNA. Suspicion of an associated neoplastic process, abscess formation that needs drainage, a poor response to antibiotic therapy, or a clinically suspected infectious process in a setting of immunosuppression may prompt an FNA, best if done under US guidance. The FNA smear pattern is purulent and shows neutrophils, fibrin strands, and variable numbers of acinar and ductal cells, which may have marked reactive changes (Fig. 5.9a, b). The most common agents are bacterial organisms, e.g., *Staphylococcus*, and FNA material must be submitted for cultures. High-grade malignant neoplasms, either primary or secondary, may show a background of neutrophils and necrosis. Caution should be

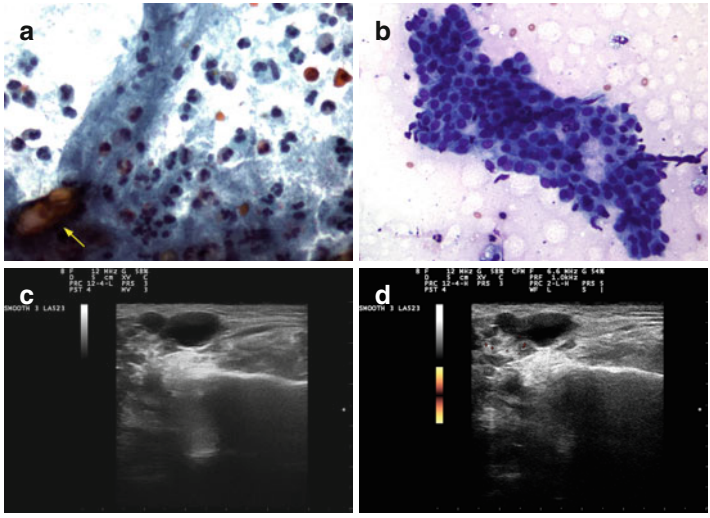

FIGURE 5.9 Parotid abscess. This patient had an episode of acute sialadenitis and developed an abscess after antibiotic therapy. A purulent pattern (**a**), stone fragments (**a**, *arrow*), and rare sheets of ductal cells with squamous metaplasia (**b**) are seen. US imaging shows a slightly irregular anechoic lesion with posterior acoustic enhancement and no vascularity by Doppler examination (**c**, **d**) (**a**, **b** MGG stain, high magnification)

exercised in diagnosing malignancy, particularly of low grade, in the presence of acute inflammation.

US features. A hypoechoic, ill-defined mass may be seen in early abscess formation; when liquefaction occurs, the mass becomes anechoic and well defined with posterior acoustic enhancement (Fig. 5.9c, d). The gland is hypervascular, and regional lymphadenopathy is often present. The enlarged gland is hypoechogenic with a heterogeneous pattern due to duct and cyst dilatation and microabscess formation.

Chronic Inflammatory Processes

The presence of chronic inflammatory cells needs clinical correlation because the majority of masses with this pattern represent salivary gland tumors with scant representation of

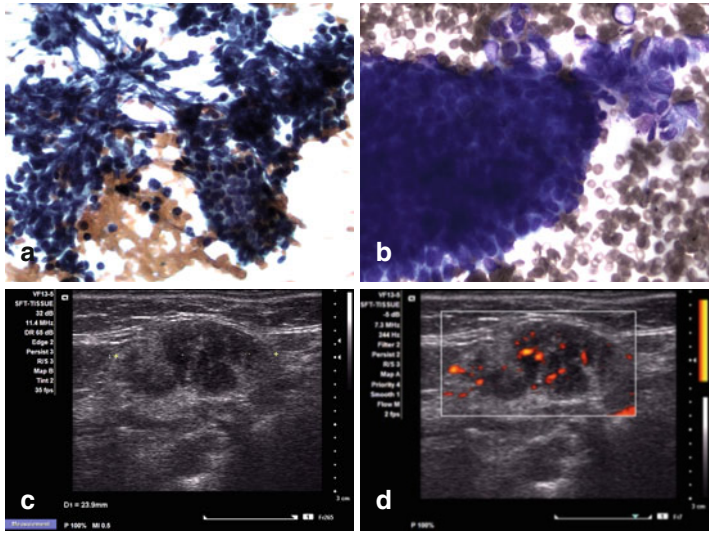

FIGURE 5.10 Chronic sialadenitis. Chronic inflammatory cells, predominantly entangled with benign salivary gland elements (**a**) and reactive aggregates of ductal cells with squamous metaplasia (**b**). Ultrasound shows a complex heterogeneous mass with anechoic foci, septae of slightly hyperechoic bands, and mild internal blood flow by Doppler examination (**c**, **d**)

epithelial cells and various degrees of nonspecific chronic inflammation, i.e., Warthin's tumor or, in some cases, intra- or peri-salivary gland lymph nodes. On US, the gland is of normal size or small, heterogeneous, and hypoechoic with multiple round hypoechoic foci. The vascularity is not increased (Fig. 5.10).

Postradiation sialadenitis produces a firm nodular and often tender salivary gland with fibrosis, acinar atrophy, and preservation of the ductal epithelial system. Smears are sparsely cellular and show fibrosis, chronic inflammatory cells, and epithelial and stromal elements with variable cytologic atypia that may pose difficulty in distinguishing this from a malignant process. The clinical history helps in the distinction. The gland is enlarged and hypoechoic in the acute phase and small, atrophic, and hypoechoic in the chronic fibrous stage.

Benign lymphoepithelial lesions present as bilateral salivary gland enlargement in patients with Mikulicz's disease or Sjögren's syndrome. Smears show a polymorphous population of lymphoid cells and epimyoepithelial islands or groups of myoepithelial cells, which may be inconspicuous. Clinical correlation is needed for consideration or support of the diagnosis. In contrast to the AIDS-related lymphoepithelial cyst, the cystic component seen in the autoimmune-related lesion is not prominent, and the normal salivary elements are almost absent. The gland is enlarged and shows normal echogenicity in the early stages. A gland with heterogeneous echotexture and multiple round hypoechoic areas or even cysts is seen in late stages. The incidence of lymphoma is greatly increased in patients with Sjögren's syndrome.

Lymphomas

The lymphomas rarely affect the salivary glands (Fig. 5.11a, b); more often is the involvement of the parotid or submandibular space lymph nodes (Fig. 5.11c). The immunophenotype as determined by flow cytometry is helpful for the diagnosis in these cases. Hodgkin lymphoma rarely involves the salivary glands, and if diagnostic Reed–Sternberg cells are not identified, these cases may be diagnosed as inflammatory process or reactive lymphoid hyperplasia. Non-Hodgkin lymphomas of low grade may be confused with reactive processes and vice versa. Occasionally, non-Hodgkin lymphoma of high grade, although often recognized as malignant, may be confused with poorly differentiated carcinoma or even small cell carcinoma.

US features. Lymphomatous deposits are markedly hypoechoic and may show through acoustic transmission with posterior acoustic enhancement the so-called "pseudocystic" appearance. The vascular pattern is increased and abnormal (Fig. 5.11d, e).

Granulomatous Processes

This pattern may be seen as a part of infectious, non-neoplastic, and neoplastic processes. Sarcoidosis, a commonly

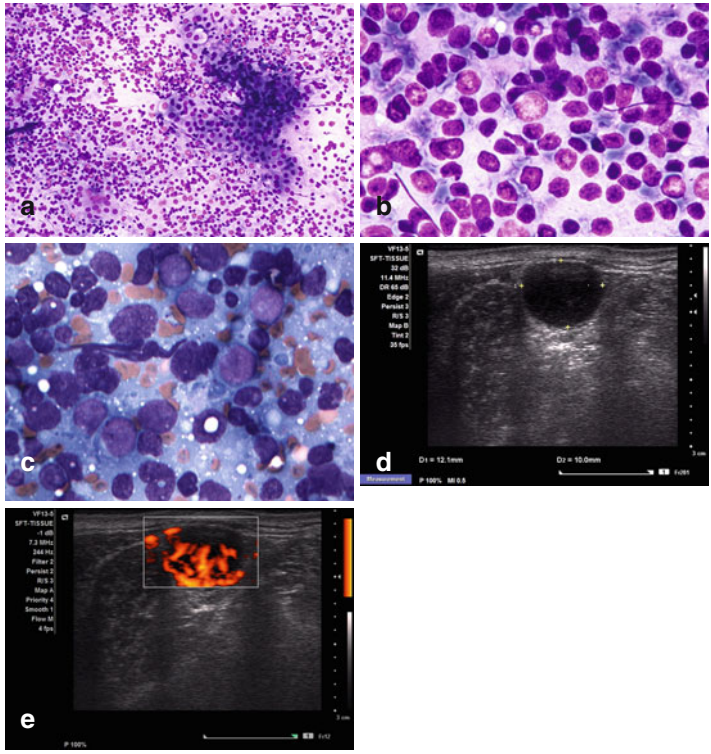

FIGURE 5.11 Mixed cell follicular lymphoma and Warthin's tumor of the parotid gland (**a**, **b**). Large B-cell lymphoma involving submandibular space lymph node (**c**). Ultrasound shows a round markedly hypoechoic lymph node with well-circumscribed margins, posterior acoustic enhancement, and chaotic internal blood flow by Doppler examination (**d**, **e**) (**a**, **b** Diff-Quik stain, medium and high magnification; **c** MGG stain high magnification)

non-necrotizing granulomatous process, may involve salivary glands or intragland lymph nodes (Fig. 5.12a, b). Necrotizing granulomatous inflammation, as in other body sites, is commonly associated with mycobacterial and fungal infections. Clinical correlation including cultures for organisms is always important. Of note, FNA material is perfectly suitable for ancillary studies, including cultures.

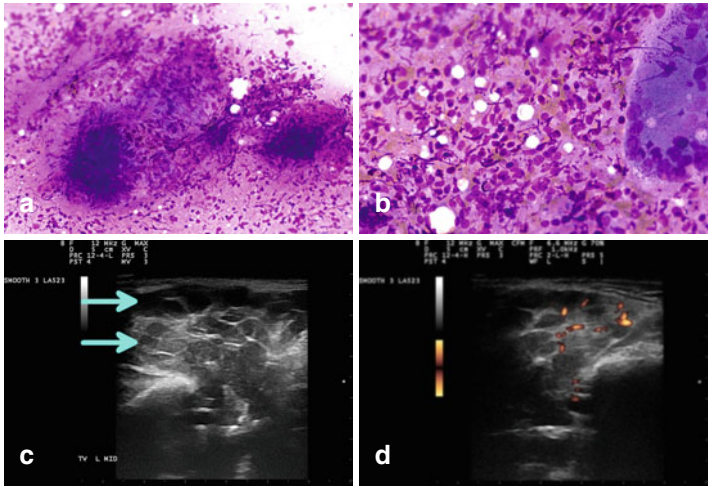

FIGURE 5.12 Sarcoidosis. Non-necrotizing granulomatous inflammation. Granulomas, chronic inflammation and tissue damage (**a**) and multinucleated giant cells are present (**b**). Ultrasound shows heterogeneous salivary gland echotexture with multiple hypechoic foci (**c**, *arrows*) vascularized septae on Doppler evaluation (**d**) (DiffQuik stain, medium and high magnification)

US features. The findings are non-specific and may show a normal or enlarged gland with diffuse hypoechogenicity or heterogeneous echotexture and lobulated gland borders (Fig. 5.12c, d).

Pattern III: Pleomorphic Adenoma (Benign Mixed Tumor), Variants, and Similar Processes

Pleomorphic Adenoma

Pleomorphic adenoma or benign mixed tumor is composed of epithelial and stromal elements. Some tumors are cellular, and others exhibit various architectural patterns that may challenge the diagnosis. Complete surgical excision with preservation of

the facial nerve is the treatment of choice. Local recurrence is rare and is often the result of incomplete resection or "spillage" of myxochondroid matrix. Complications include malignant transformation, particularly in large and long-standing tumors and in the so-called metastasizing pleomorphic adenoma.

Clinical findings. Pleomorphic adenoma is the most common tumor of the salivary glands and occurs predominantly in the tail of the parotid gland. It is rare in the sublingual glands. It is the most frequent tumor of the parapharyngeal space, followed by peripheral nerve sheath tumors. It has a slight female predominance, with variable age presentation, usually occurring in adults and the elderly. Familial occurrence is rare. Bilateral or multiple tumors are uncommon. Tumors are slowly growing over years, and except for compressive mechanical symptoms, patients are almost always asymptomatic. Tumors are firm, well circumscribed, with regular and lobulated borders, and of variable size.

Histopathology. All tumors have a capsule of variable thickness and may be non-visible, particularly in cases with abundant myxoid matrix.

Typical pleomorphic adenomas have a mixture of ductal epithelial, myoepithelial, and stromal elements. The epithelial component may show variable architectural patterns including trabecular, papillary, tubular, solid, or cystic, even within the same tumor. The islands and tubules have an inner layer of cuboidal/columnar/flattened epithelial cells and outer myoepithelial cell layer(s). The stromal component is myxoid, chondroid, or fibro-osseous alone or mixed. Crystalloids may also be present in the background. Squamous elements in the form of pearls or squamous cells as well as mucous cells, clear cells, spindle cells, plasmacytoid cells, sebaceous cells, oncocytic cells, calcification, and adipose tissue may be seen. Degenerative changes may be seen spontaneously or after FNA and include squamous metaplasia, reactive cellular changes, necrosis, and infarction.

Cellular pleomorphic adenomas may be rich in epithelial or myoepithelial cells, but every case shows the typical component described above, although it may be limited. There may be large atypical cells and rare non-atypical mitoses; as long as these features are focally present, they do not signify malignancy.

Most tumors are diagnosed without difficulty; however, those with a predominant cellular epithelial or myoepithelial component or those with variable architectural patterns must be recognized and distinguished from other tumors such as polymorphous low-grade adenocarcinoma when involving minor salivary glands or adenoid cystic carcinoma in the major salivary glands. Pleomorphic adenomas with predominant rich myxoid stroma must be distinguished from mesenchymal tumors, including but not limited to myxoid lipoma, myxoid neurofibroma, and myxoma.

Immunoprofile. Epithelial cells show keratin, CEA, and EMA positivity. Myoepithelial cells are positive for calponin, p63, actin, vimentin, S-100 protein, CD10, glial fibrillary acid protein, and keratin but are CEA and EMA negative. Podoplanin, a myoepithelial cell marker has been shown to be positive on the cell border and in the external periphery of the cells in pleomorphic adenoma and other salivary gland tumors with myoepithelial differentiation.

Molecular profile. Most pleomorphic adenomas have karyotypic abnormalities including 8q12 rearrangements, 12q14–15 rearrangements, or sporadic clonal changes. The 8q12 and the 12q14–15 abnormalities activate the target genes *PLAG1* and *HMGA2*, respectively, producing fusions that are specific and diagnostic for these tumors.

FNA findings. Ductal cells are small, cuboidal, and bland appearing and can be single or form sheets, acini, tubules, or branching aggregates (Fig. 5.13a). Cells show round, regular nuclei with fine chromatin and inconspicuous nucleoli and may have mild to moderate pleomorphism (arrows Fig. 5.13b); occasional intranuclear inclusions may be present. The epithelial component may have cystic change and squamous, clear cell, mucinous, oncocytic, and sebaceous metaplasia (Fig. 5.13c). Myoepithelial cells are usually dissociated or in small aggregates and show plasmacytoid or spindle shapes and may have moderate pleomorphism; they may be mistaken for hematopoietic cells (Fig. 5.13d). Myoepithelial cells appear faint with poorly defined cell borders when admixed with the stroma (Fig. 5.13e). The chondromyxoid matrix, in air-dried Romanowsky-stained slides, is characteristic and

appears metachromatic, dense, and fibrillary; the last feature is particularly visible in the frayed edges (Fig. 5.13e, f). The matrix is less conspicuous with Papanicolaou stain and appears pale and gray; and myoepithelial cells may appear stellate or spindle. Thus, Romanowsky-stained slides are advantageous for detection of small amounts of stromal elements, and they lower the possibility of an incorrect diagnosis. Necrosis and cellular atypia secondary to infarction may rarely be associated with prior FNA.

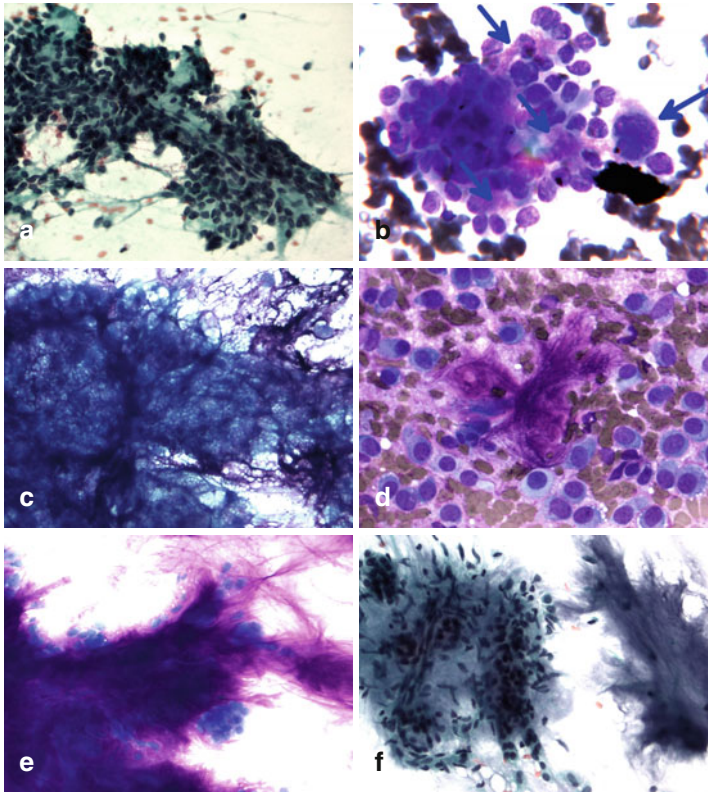

FIGURE 5.13 Benign mixed tumor. Cytologic features (**a–f**). Ultrasound characteristics (**g–l**) (**a–f** Papanicolaou and MGG stains, medium and high magnification)

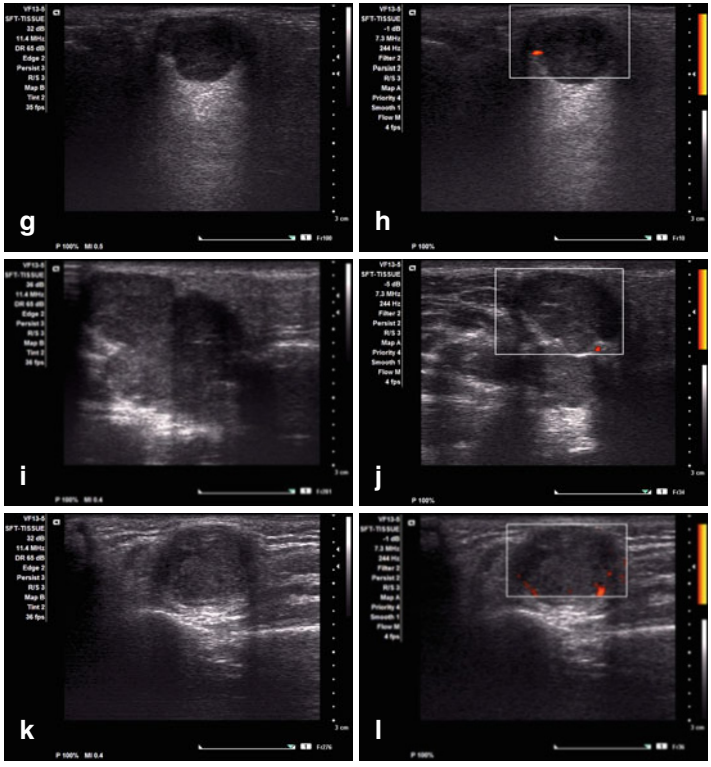

FIGURE 5.13 (continued)

It should be emphasized that finding fibrillary stroma overrides any ductal or myoepithelial cell atypia that may suggest malignancy including carcinoma ex-pleomorphic adenoma, which should be carefully considered due to its rarity particularly in the absence of facial nerve-related clinical findings.

Myoepithelioma should be considered when myoepithelial cells predominate. However, because the stroma is the most conspicuous element in the pleomorphic adenoma pattern, the differential FNA diagnosis includes mucoepidermoid carcinoma, polymorphous low-grade adenocarcinoma, and adenoid cystic carcinoma. Pleomorphic adenoma may resemble

mucoepidermoid carcinoma based on the presence of marked mucinous metaplasia, foam cells secondary to cystic change, and metaplastic squamous cells. Finding less dense stroma that, on careful examination appears fibrillary, is helpful for reaching the correct diagnosis.

Cellular pleomorphic adenoma with a cylindromatous pattern and limited stromal elements should be distinguished from adenoid cystic carcinoma and will be discussed in the section "small epithelial cell pattern." Except for the proclivity to affect minor salivary glands instead of the parotid gland and the perineural invasion seen in polymorphous low-grade adenocarcinoma, both polymorphous low-grade adenocarcinoma and pleomorphic adenoma have stromal and epithelial cell similarities that make FNA distinction difficult.

US features. A round or oval well-defined hypoechoic solid mass with a lobulated or bosselated surface is usually located in the superficial portion of the parotid gland. The mass is homogeneous and often displays a "through" transmission with posterior acoustic enhancement ("pseudocystic" appearance). Power Doppler often demonstrates peripheral blood flow. Irregular ill-defined margins and heterogeneity raise the possibility of malignancy. Cystic and hemorrhagic degeneration is usually not seen; however, it may be observed in tumors larger than 3 cm. Calcifications may occur in long-standing tumors (Fig. 5.13g–l).

Recurrent pleomorphic adenoma almost always occurs in or around the surgical excision site. Single or multiple nodules with smooth and well-defined borders, homogeneous echotexture, posterior acoustic enhancement, and peripheral vascularity may be present in these recurrent tumors.

Atypical Pleomorphic Adenoma

The atypical features of this tumor include high cellularity, cellular pleomorphism, increased mitoses, and/or necrosis. These features may suggest malignancy and should prompt extensive tissue sampling; however, they should not be mistaken for malignancy (Fig. 5.14).

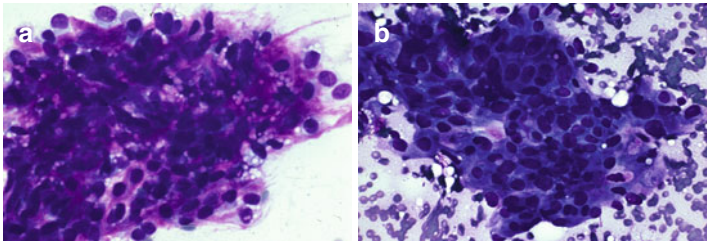

FIGURE 5.14 Benign mixed tumor with atypia and sebaceous (**a**) and squamous (**b**) metaplasia (Diff-Quik stain, high magnification)

Metastasizing Pleomorphic Adenoma

Deposits of otherwise typical pleomorphic adenoma may be seen occasionally in the lungs, mimicking pulmonary hamartoma, or in the bone, mimicking chondrosarcoma or myxoid malignant fibrous histiocytoma. Clinical and radiographic findings are required for adequate interpretation of the FNA findings.

Polymorphous Low-Grade Adenocarcinoma

Characteristically, this tumor shows bland cyto- and histomorphology, shows variable histologic patterns, and has low metastatic potential.

Clinical findings. This tumor originates almost exclusively in the minor salivary glands of the oral cavity, particularly the palate. It is more common in women and frequently occurs in the sixth to eighth decade of life. The patient has a non-tender mass that can last for months to years.

Histopathology. This well-circumscribed unencapsulated tumor shows various growth patterns, including a solid, cribriform, glandular, tubular, cystic, papillary, trabecular, or single cell linear pattern. Tumor cells are bland-appearing cuboidal and of medium size with round to elongated nuclei, granular fine chromatin, and inconspicuous nucleoli. Nuclear pleomorphism, necrosis, and mitoses are rare. The stroma is hyaline or mucoid and may have areas of hemorrhage.

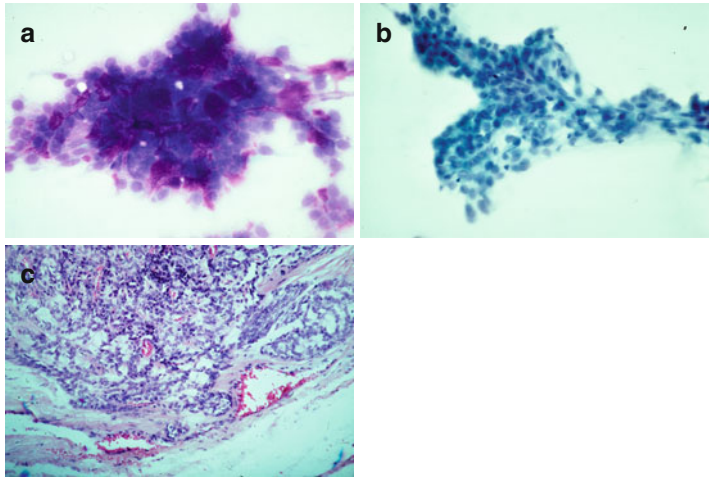

FIGURE 5.15 Polymorphous low-grade adenocarcinoma. Pseudopapillary aggregates with myxoid matrix are present (**a**). There are fine capillaries surrounded by bland-appearing epithelial cells (**b**). Histologic findings show glandular, cribriform, and trabecular patterns (**c**) (**a** MGG stain, high magnification; **b** Papanicolaou stain, medium magnification; **c** hematoxylin and eosin stain, medium magnification)

Squamous, oncocytic, or mucinous metaplasia may be seen as well as intratubular calcifications. Pseudoepitheliomatous hyperplasia of the overlying epithelium may be present.

Immunoprofile. Neoplastic cells show positive immunoreactivity for CEA, keratin, S-100 protein, vimentin, EMA, actin, CD117, Bcl-2, and galectin-3.

Molecular profile. Alterations of the 8q12 chromosome band, 12q rearrangements, and clonal t(6:9)(p21;p22) have been observed.

FNA findings. Smears are often of high cellularity and show epithelial cells, myoepithelial cells, and myxoid matrix. The epithelial cells are seen in aggregates or sheets and occasionally as branching pseudopapillary aggregates. Cells are cuboidal to spindle shaped with round to oval uniform nuclei, fine chromatin, inconspicuous nucleoli, and dense cytoplasm (Fig. 5.15). The cell features are important for distinguishing

this tumor from pleomorphic adenoma that has plasmacytoid myoepithelial cells or adenoid cystic carcinoma that shows more basaloid hyperchromatic cells and lacks cell pleomorphism or necrosis.

Pattern IV: Warthin's Tumor and Similar Processes

Warthin's Tumor

Warthin's tumor is the second most common salivary gland tumor, has cigarette smoking as the main risk factor, is more prevalent after the fourth decade of life, involves almost exclusively the parotid gland, is bilateral in 10 % of cases, and is slightly more common in men. Complete surgical excision is the treatment of choice.

Clinical findings. Tumors are softer than pleomorphic adenomas and may even be fluctuant when predominantly cystic. Patients are usually asymptomatic. Transformation to epithelial or lymphoid malignancy is exceedingly rare.

Histopathology. The epithelial component is oncocytic, arranged as a double layer with inner columnar and outer smaller cuboidal cells that decorate cystic, glandular, or papillary projections. The lymphoid elements are predominantly mature and may exhibit germinal centers. Mucous and goblet cells as well as sebaceous glands may be seen.

Immunoprofile. Epithelial cells show positivity for keratin and EMA and are negative for S-100 protein, p63, calponin, actin, and GFAP. Lymphoid cells lack light-chain restriction and are positive for mature B- and T-cell markers.

Molecular profile. The majority of these tumors show a normal karyotype. Approximately 10 % of tumors have cytogenetic abnormalities; 6p rearrangement and 11q;19p translocations are the most common and consistent abnormalities in this tumor.

FNA findings. Smears may show three components in various proportions: oncocytic cells, lymphocytes, and cyst fluid.

Oncocytic cells often occur in cohesive flat sheets showing abundant cytoplasm, well-defined cytoplasmic borders, round nuclei, and conspicuous nucleoli. The cytoplasm is granular and eosinophilic when stained with Papanicolaou stain or dense in air-dried Romanowsky-stained preparations (Fig. 5.16a, b). Sebaceous, mucinous, or squamous metaplasia may be seen (Fig. 5.16c). The lymphoid cells are usually small and may be scattered in the smear background or tangled among themselves or with the epithelial elements (Fig. 5.16d). The cystic component shows debris admixed with variable numbers of macrophages and lymphocytes (Fig. 5.16e). Cholesterol crystals may be seen.

In the presence of a lymphoid-rich FNA, chronic inflammation, reactive lymphoid hyperplasia, or even small cell-type non-Hodgkin lymphoma may be differential diagnostic considerations. Flow cytometry is helpful in questionable cases. Cyst content characteristics are highly suggestive of Warthin's tumor; however, the diagnosis cannot be made without the presence of oncocytic cells; then repeat FNA under US guidance should be performed for sampling of the solid component. Mucoepidermoid carcinoma may be considered when the oncocytic epithelium is not prominent, and squamous metaplasia is identified in a background of cyst fluid that may be mistaken for mucin (Fig. 5.16f). Cystic squamous cell carcinoma may be considered when atypical squamous metaplasia is apparent in a background of cystic elements. When oncocytic cells predominate and the cyst fluid is not prominent, the differential diagnosis includes oncocytic neoplasms, i.e., oncocytoma or oncocytic papillary cystadenoma, among others. Cells of acinic cell carcinoma may be difficult to differentiate from those of oncocytic neoplasms, particularly Warthin's tumor, because both lymphocytes and cystic fluid may be present in these tumors. In contrast to the fine granularity of Warthin's tumor, the coarse cytoplasmic zymogen granules of acinic cell carcinoma are more prominent in cell block slides. Necrosis, infarction, reactive changes, and hemorrhagic and granulation tissue may be encountered as a result of FNA sampling.

US features. This tumor is usually a well-circumscribed round or ovoid hypoechoic mass which is heterogeneous with solid and cystic areas or multiseptated with spongiform cystic architecture. This US pattern is highly suspicious for Warthin's tumor, but is not common. Power Doppler may show variable vascularity, particularly in the septa of the tumor (Fig. 5.16g–l).

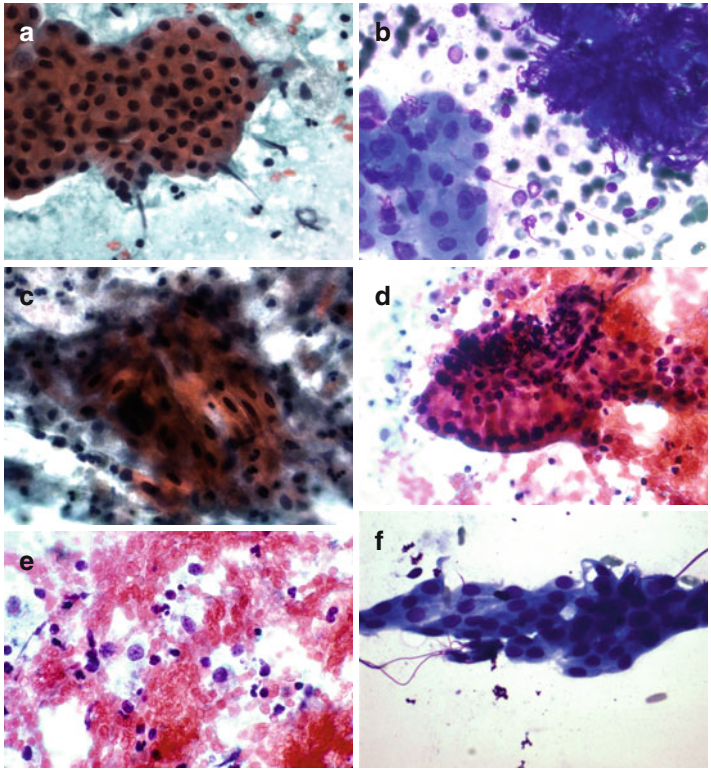

FIGURE 5.16 Warthin's tumor. Cytologic features (**a–f**). Ultrasound characteristics (**g–l**) (**a–f** Papanicolaou and MGG stains, medium and high magnification)

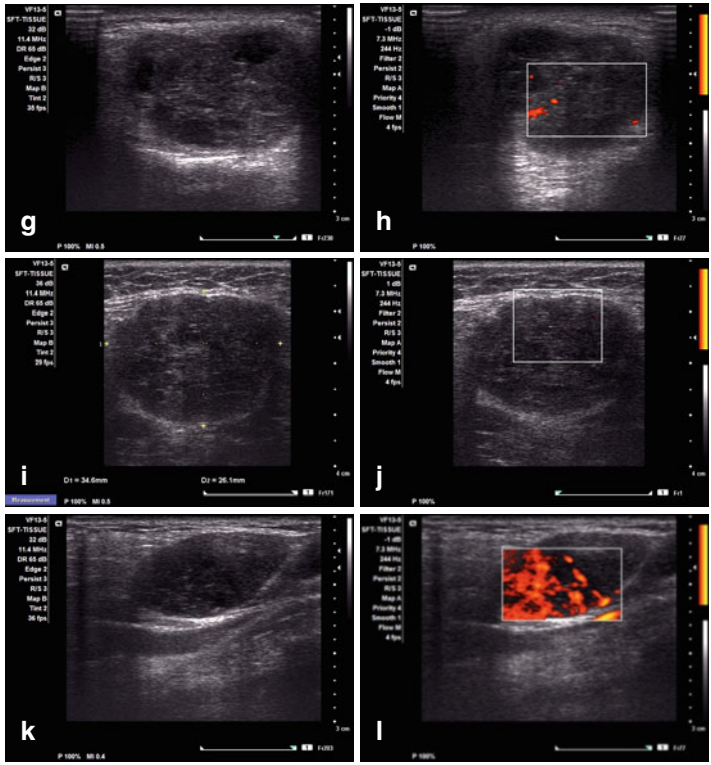

FIGURE 5.16 (continued)

Pattern V: Cystic Pattern and Similar Processes

The cyst contents obtained by FNA may be broadly classified as non-mucinous and mucinous. Each of these categories has a broad differential diagnosis that includes primary nonneoplastic and neoplastic benign or malignant lesions. It should be remembered that cystic change may also be the result of degeneration in solid tumors. The differential diagnosis is narrowed when other cellular or noncellular elements are visualized.

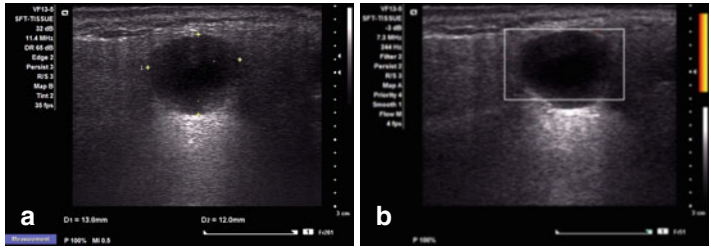

Figure 5.17 Parotid gland cyst. US shows a round nodule with well-defined margins, anechoic pattern, posterior acoustic enhancement, and no vascularity by Doppler exam

US features. Regardless of the etiology, cysts have similar characteristics, including well-defined edges, thin walls, anechoic pattern, posterior acoustic enhancement, and no vascularity (Fig. 5.17). If the cyst becomes infected, the wall becomes thick and there is internal debris.

Non-mucinous Cystic Lesions

Crystals in Cystic Lesions

Cysts may contain crystals, i.e., α-amylase and tyrosine.

Alpha-amylase crystals are not associated with malignant processes. Smears show polyhedral and multifaceted structures of variable size and thickness commonly associated with scant epithelial elements, predominantly oncocytic cells (Fig. 5.18). These crystals have been observed predominantly in cystic spaces lined with metaplastic oncocytic cells in Warthin's tumor, oncocytic papillary cystadenoma, pleomorphic adenoma, sialadenitis, and sialolithiasis. The crystals may be a product of oncocytic cell secretion.

Tyrosine crystals, on the contrary, have been found in malignant and nonmalignant neoplastic processes, more frequently in black patients.

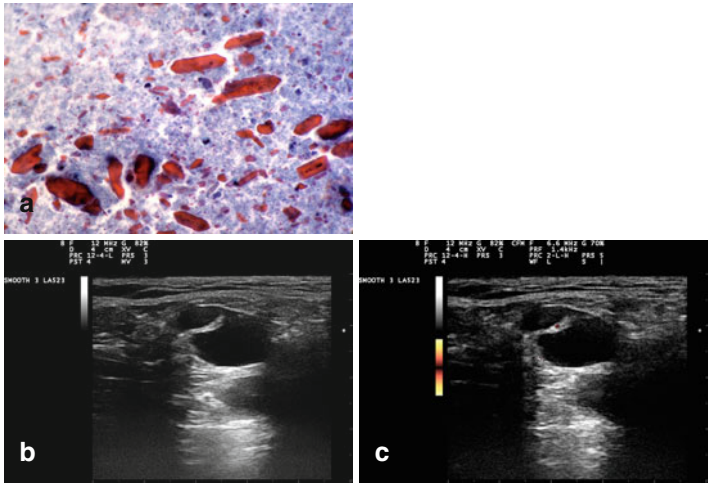

FIGURE 5.18 Parotid gland cyst with alpha-amylase crystals. Smear shows characteristic polyhedral and multifaceted crystals (**a**). US shows a septated cyst with posterior acoustic enhancement (**b**) and minimal vascularity in the septum by Doppler exam (**c**) (**a** SurePath preparation, high magnification)

Lymphoepithelial Cysts

This AIDS-related process affects principally the parotid gland, unilaterally or bilaterally, and shows hyperplastic lymphoid tissue lining cystic structures, which may show squamous, columnar ciliated or non-ciliated, or mucinous epithelium or even sebaceous glands (Fig. 5.19a). Cytologic findings include epithelial cells of the types described, polymorphous lymphoid cells, and a cystic background (Fig. 5.19b, c). The differential diagnosis depends on the predominant elements identified; however, clinical correlation is important, considering that reactive lymphoid hyperplasia and lymphoepithelial cysts are more common than malignant lymphoma, and Kaposi's sarcoma, the most common

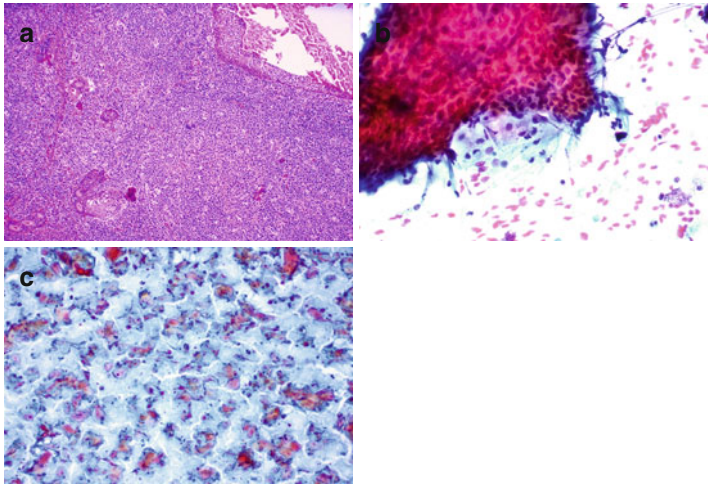

FIGURE 5.19 Lymphoepithelial cyst. Histologic section showing reactive follicular hyperplasia and a cyst lined with benign squamous epithelium (**a**). Squamous cells in complex aggregates and single are seen along with lymphocytes (**b**, **c**) (**a** hematoxylin and eosin stain, low magnification; **b**, **c** Papanicolaou stain, low and medium magnification)

malignancies in patients with AIDS. Some lymphoepithelial cysts may have a complex echotexture with solid and cystic areas resembling tumors.

Mucinous Cystic Lesions

Obstructive Sialopathy

These processes may be the result of fibrosis, adjacent masses, or sialolithiasis obstructing the ductal system, causing retrograde dilatation and mucin accumulation. As a result, acinar atrophy, chronic inflammation, and occasionally acute inflammation may occur. The lining epithelium of the dilated ducts is usually flattened or may show squamous, mucinous, or ciliated metaplasia. Foreign body reaction and stromal reactive

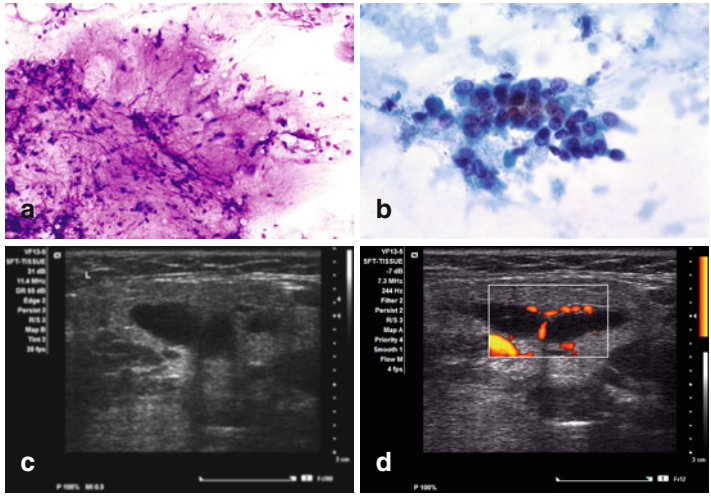

FIGURE 5.20 Obstructive sialopathy. Squamous metaplasia, chronic inflammation, and cyst contents were the findings in this submandibular gland lesion (**a**, **b**). US shows cystic cavity surrounded by a thick wall, vascular by Doppler examination (**c**, **d**) (**a**, **b** Papanicolaou stain, high magnification)

changes may occur if there is rupture of the dilated duct. Cytology preparations are similar, if not identical to those of a low-grade mucoepidermoid carcinoma (Fig. 5.20).

Sialolithiasis

This process is more common in women than in men and affects predominantly the submandibular gland, mainly as a unilateral lesion. Most calculi are single; 90 % of submandibular gland and 10 % of parotid gland stones are radiopaque. Clinically, patients classically present with pain at mealtime; however, they may be asymptomatic and have a firm mass suggestive of malignancy.

The FNA diagnosis can be made in the presence of stone fragments that may be associated with cell metaplasia,

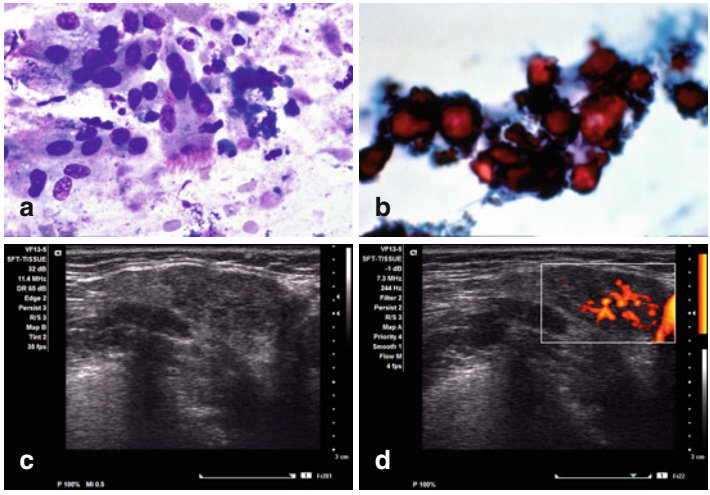

FIGURE 5.21 Sialolithiasis. Ciliated metaplasia and crystals are present in a mucoid background (**a**, **b**). US shows a hypoechoic area with lobulated edges and high vascular blood flow by Doppler exam (**c**, **d**) (**a**, **b** Papanicolaou stain, high magnification)

including ciliated columnar cells, which may be interpreted as a congenital cyst when stone fragments are not evident. The background is mucinous, with debris, and may be sparsely cellular (Fig. 5.21a, b).

The main differential diagnosis is low-grade mucoepidermoid carcinoma in the absence of stone fragments and ciliated metaplasia and in the presence of squamous metaplasia, foam cells, and reactive, bland ductal cells. In cases where mucus is only present, the FNA diagnosis of "mucinous smear pattern" is suggested, followed by a comment addressing the differential diagnosis.

US features. The gland appears enlarged and hypoechoic due to ectasia and has variably dilated ducts. Duct dilatation may be usually seen, with the duct stone showing a hyperechoic rim and posterior acoustic shadowing. Parenchymal stones can also be identified. Cyst and abscess formation may also be seen (Fig. 5.21c, d).

Low-Grade Mucoepidermoid Carcinoma

Mucoepidermoid carcinoma (MEC) is a malignant tumor composed of mucin-producing epithelium, squamous cells, intermediate cells, and mucus. Wide local surgical excision with preservation of the facial nerve is the treatment of choice.

Clinical findings. This is the most common salivary gland malignant neoplasm in both adults and children. It is more common in women than in men and occurs principally in the fifth decade of life, although it may occur in children in the second decade of life. It affects predominantly the parotid gland, the palate being the most frequent minor salivary site. The low-grade tumors are slowly growing and usually are asymptomatic, in contrast to the high-grade type, which are fast growing and cause pain. Low-grade tumors have an excellent prognosis, whereas high-grade ones have a poor prognosis.

Histopathology. The tumors are often cystic. Mucus cells usually compose <10 % of the tumor and are round and large and show well-defined cytoplasmic borders, clear or foamy cytoplasm, and small, dark eccentric nuclei. Epidermoid cells have a polygonal shape, dense eosinophilic cytoplasm, well-defined cytoplasmic borders, and vesicular nuclei. Keratinization is rare except in inflamed tumors. Intermediate cells may be small basal or large polygonal cells. Basal cells have round/oval nuclei and scant eosinophilic cytoplasm. Large polygonal cells are round to oval with more abundant cytoplasm. Clear cells may be present and are occasionally prominent, as in the rare clear cell variant of MEC. Oncocytic cells are seen in the oncocytic variant of MEC. Hyalinized or sclerosed stroma is seen in sclerosing MEC. Psammomatous MEC is another variant.

The histologic grading is fundamentally based on the predominance of the cystic component (low-grade MEC) or the solid component (high-grade MEC). Cellular pleomorphism, necrosis, mitosis, and hemorrhage are usually absent in low-grade tumors. The differential diagnosis depends on the tumor grade and includes obstructive sialopathy, necrotizing sialometaplasia, cystadenoma, and carcinomas including metastasis.

Immunoprofile. Epidermoid, intermediate, and columnar cells are cytokeratin and EMA positive. Mucous cells are cytokeratin and EMA negative. CK5/CK6 and p63 highlight squamous derivation, and PAS demonstrates mucus. Oncocytic variant is strongly positive for p63.

Molecular profile. Mutations are found mainly in high-grade tumors. The t(11;19)(q12;p13) in MEC is highly specific and results in fusion of the MEC translocated gene-1 or *MECT1* gene and the mastermind-like gene family or *MAML2* gene. The MECT1–MAML2 fusion transcript, which is present in more than half of all MECs, is associated with lower histologic grades and improved survival, suggesting both diagnostic and prognostic roles in clinical management. The translocation has not been seen in other salivary gland malignancies and can potentially be of diagnostic value using a FISH-based approach in FNA material, when MEC particularly of low grade is suspected.

FNA findings. The smear pattern is similar to that seen in obstructive sialopathy (Fig. 5.20a, b). Smears are acellular or hypocellular, and the background shows abundant mucin that, in contrast to pleomorphic adenoma, does not appear fibrillary and does not stain as intensely. Cellular elements appear singly or in aggregates (Fig. 5.22a, b). The epidermoid cells are bland appearing, and the mucous cells are plump with vacuolated cytoplasm indistinguishable from macrophages, well-defined cytoplasmic borders, and eccentric nuclei displaced by the cytoplasmic mucin (Fig. 5.22c). The mucous cells are fewer than the epidermoid cells. Intermediate cells are bland appearing and have moderate amounts of cytoplasm.

US features. Low-grade MEC is usually hypoechoic and well defined, and it shares US features with benign salivary gland tumors (Fig. 5.22d, e). In contrast, high-grade malignancies may be frankly infiltrative. Large tumors have a complex heterogeneous echotexture reflecting intratumoral necrosis or hemorrhage. Malignant tumors are more likely to have a disorganized vascular flow and have regional neck lymph node metastases.

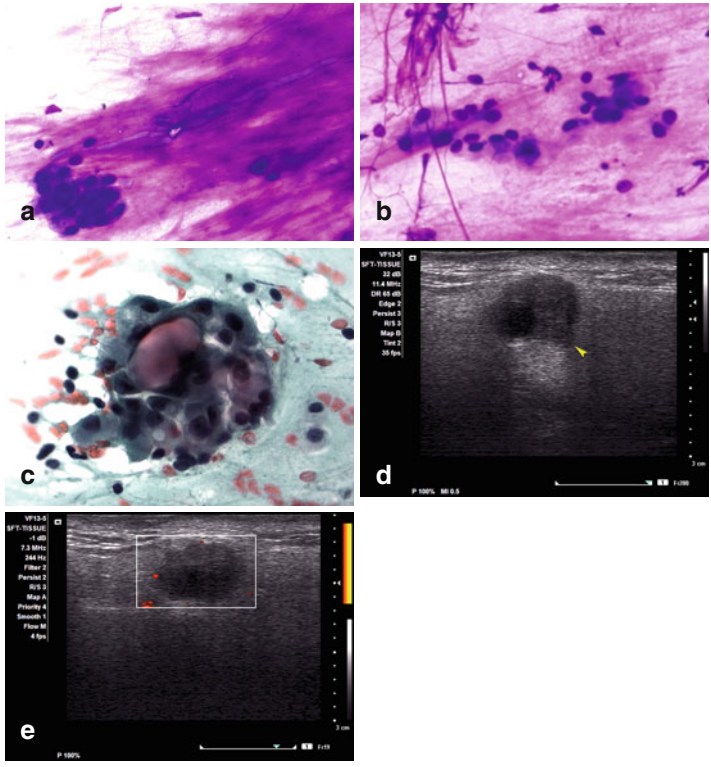

FIGURE 5.22 Low-grade mucoepidermoid carcinoma. Abundant mucus, scattered small cell groups, intermediate-type squamous cells, and few mucin-producing cells are characteristic, although not diagnostic findings, of this tumor (**a**–**c**). US features are not specific and overlap with those of benign cysts and tumors including marked hypoechogenicity and well-defined borders (**d**, **e**). The *arrowhead* points to an area of extracapsular invasion (**a**, **b** Diff-Quik stain, high magnification; **c** Papanicolaou stain, high magnification)

Pattern VI: Small Epithelial Cell Pattern

Various primary salivary neoplasms as well as dermal, adnexal, and even metastatic deposits should be considered in the differential diagnosis of this cytologic pattern. Primary

salivary gland neoplasms include monomorphic adenoma, pleomorphic adenoma with scanty stroma, adenoid cystic carcinoma, and rarely, primary small cell carcinoma and lymphoepithelioma-like carcinoma. Dermal eccrine cylindroma and pilomatrixoma, infiltrative or metastatic basal cell carcinoma, metastatic neuroendocrine carcinoma of the skin or lung, and lymphomas must be considered in light of the clinical findings. Differentiating monomorphic adenoma from adenoid cystic carcinoma may be one of the most difficult diagnostic problems in salivary gland cytology.

Monomorphic Adenoma (Basal Cell Adenoma)

This tumor is composed of small, uniform basaloid cells and absence of the myxochondroid stroma seen in pleomorphic adenoma. Cytologically, this tumor is often indistinguishable from pleomorphic adenoma, with scant stroma and adenoid cystic carcinoma. Complete surgical excision is the treatment of choice. Local recurrences are unusual.

Clinical findings. This rare tumor affects predominantly the parotid gland of adults, with no sex predilection. Patients often have an asymptomatic mass present for a variable period ranging from months to years. Superficial lobe tumors are detected earlier; thus, the size usually is <3 cm. Larger tumors are located in the deep lobe and tend to have cystic degeneration.

Histopathology. Tumors of major glands are encapsulated, whereas those of minor glands are often uncapsulated, although well circumscribed. Cells are columnar or cuboidal and are arranged in tubular, solid, trabecular, or membranous patterns of growth. All patterns, but in particular the solid pattern, may show squamous horns or eddies, and the membranous pattern shows thick eosinophilic hyaline membranes, which are reduplicated basement lamina similar to those of dermal cylindroma.

Immunoprofile. In the tubular component, epithelial cells are cytokeratin, EMA, and CEA positive. The myoepithelial cells are CD10, calponin, p63, actin, and S-100 protein positive.

Molecular profile. Loss of heterozygosity 16q12–13, a region related to the cylindromatosis gene *CYLD*, has been found. Trisomy of chromosome 8 and t(7;13) have also been reported.

FNA findings. Smears are cellular and show numerous blue cells and variable amounts of collagenous stroma that appears metachromatic on Romanowsky stains (Fig. 5.23a). Cellular dissociation and single cells may be numerous. The membranous basal cell adenoma shows features identical to those of adenoid cystic carcinoma, and the distinction between the two is almost impossible. When cellular complex aggregates with little or no stroma are the predominant pattern, the distinction from the solid (anaplastic) type of adenoid cystic carcinoma may be extremely difficult. The identification of spindle cells and capillaries within the arborizing collagenous stroma is useful for the correct identification of the tumor (Fig. 5.23b). Also, the stroma cell interface is fuzzy and fibrillary, with a subtle interconnection between the two instead of the sharp interface often seen in adenoid cystic carcinoma (Fig. 5.23c). However, adenoid cystic carcinoma may show a fibrillary desmoplastic stroma produced in the areas of invasion that is indistinguishable from the stroma of basal cell adenoma. The difficulty of the distinction is even more difficult in the solid type of adenoid cystic carcinoma that shows limited amounts of the characteristic globular cylindromatous metachromatic extracellular matrix. The well-demarcated cylinder cell interface may not be prominent in this type.

US features. Superficial tumors are solid and often round or oval, well circumscribed, and hypoechoic, with a homogeneous echotexture (Fig. 5.23d, e). Deep tumors are larger, often round and well circumscribed, and hypoechoic, with a variably heterogeneous echotexture due to cystic change, particularly in tumors measuring >3 cm (Fig. 5.23f, g). Almost all tumors show posterior acoustic enhancement.

Adenoid Cystic Carcinoma

This basaloid malignant tumor is composed of epithelial and modified myoepithelial cells and varying amounts of globular cylindromatous matrix. Surgery is the treatment of choice,

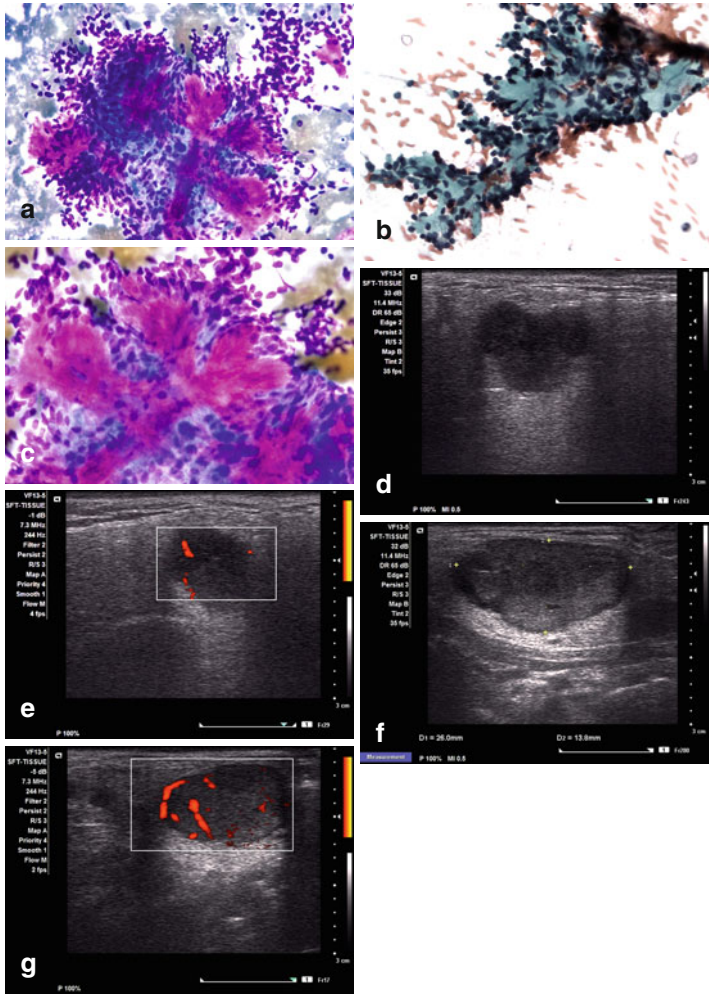

FIGURE 5.23 Monomorphic (basal cell) adenoma. Cytologic findings (**a**–**c**). Ultrasound features are not specific and overlap with those seen in benign mixed tumors including lobulated margins, hypoechogenicity with posterior acoustic enhancement (**d**, **e**), and slightly heterogeneous echotexture in larger tumors (**f**, **g**) (**a**, **c** Diff-Quik stain, high magnification; **b** Papanicolaou stain, medium magnification)

and radiation therapy may be considered in unresectable and/or deeply invasive tumors.

Clinical findings. This tumor comprises 10 % of salivary gland neoplasms and affects major and minor salivary glands. It occurs predominantly in adult and old individuals who present with a slow-growing mass with associated local pain, paresthesia, or even facial nerve paralysis. The prognosis is poor, and the outcome is usually fatal.

Histopathology. This infiltrative unencapsulated tumor has cells arranged in tubular, cribriform, and solid architectural patterns that are present in various proportions in the tumor. The lumens are filled with hyaline mucoid material. Perineural invasion is commonly seen.

Immunoprofile. No markers are specific for this tumor. Epithelial cells are keratin, CEA, and EMA positive. The myoepithelial cells are CD10, calponin, p63, actin, and S-100 protein positive. The tumor is reported to be positive for CD117 and bcl-2. Ki-67 immunostain may be helpful for distinguishing this tumor from polymorphous low-grade adenocarcinoma. The extracellular material is PAS and mucicarmine positive. Other biomarkers expressed in adenoid cystic carcinoma include p53, EGFR, and MYB.

Molecular profile. The t(6;9)(q22-23;p23-24) translocation in adenoid cystic carcinoma results in fusion and activation of the *MYB* gene at 6q22-23 and the *NFIB* gene at 9p23-24. The *MYB–NFIB* fusion transcript, present in at least one third of salivary gland adenoid cystic carcinomas, can be detected by new reverse transcription polymerase chain reaction screening methods and FISH, and has emerged as a potential therapeutic target. Frequently, there is overexpression of the c-kit protein; however, no *c-kit* gene mutations have been shown and no response to imatinib mesylate therapy has been reported.

FNA findings. Smears are cellular, and, depending on the histologic pattern, the cellular elements may be complex tridimensional, glandular, trabecular, and solid, composed of small blue cells (Fig. 5.24a). Cell dissociation is usually prominent,

and numerous stripped nuclei are present in the background. The cells are uniform, and nuclear features are usually bland-appearing with small nucleoli and do not show features of malignancy (Fig. 5.24b).

The stroma seen in adenoid cystic carcinoma is of two types: (1) the classic cylindromatous globular stroma resulting from basal membrane reduplication is acellular and avascular and has a sharp separating edge from the surrounding blue cells (Fig. 5.24c, d) and (2) the desmoplastic tumor stroma seen in the areas of invasion is fibrillary with fuzzy borders and interdigitates with the surrounding blue epithelial cells in a fashion similar to that seen in basal cell adenoma (Fig. 5.24e).

Two important features that may be seen in smears are necrosis and atypical mitoses that would favor the diagnosis of adenoid cystic carcinoma over basal cell adenoma; however, these features are found infrequently. Thus, considering the overlapping FNA cytology between these two tumors, the Swedish school of cytology recommends, based on its vast experience, that even in the presence of classical cytologic features of adenoid cystic carcinoma, such a conclusive diagnosis should be made only in the presence of symptoms and signs of facial nerve damage.

Neoplasms that have a cylindromatous pattern and mimic adenoid cystic carcinoma include pleomorphic adenoma, basal cell adenoma, epithelial–myoepithelial carcinoma, and polymorphous low-grade adenocarcinoma. Pilomatrixoma with prominent basaloid cell representation and scanty squamous ghost cells and calcific matter is another tumor that resembles solid adenoid cystic and basal cell adenoma. Clinical features and careful search for additional cytologic features are helpful for reaching the diagnosis. Likewise, basal cell adenocarcinoma primarily to the salivary gland and basal cell carcinoma of dermal origin show cytologic features very similar to those of solid adenoid cystic carcinoma and basal cell adenoma. Mitoses and necrosis, when present, help in the distinction of a malignant process from basal cell adenoma. Cytologic diagnosis of the specific type of malignancy is often less than impossible.

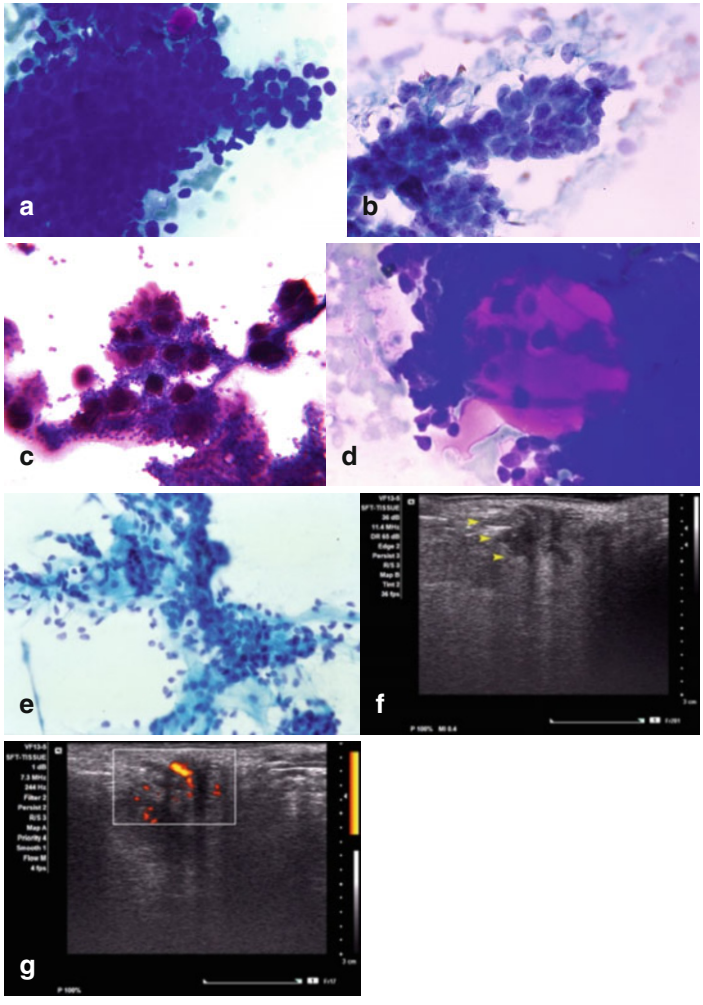

FIGURE 5.24 Adenoid cystic carcinoma. Cytologic findings (**a**–**e**). Ultrasound images show a mass with ill-defined margins, heterogeneous echotexture, and infiltrating borders (*arrowheads*); the needle length is seen emerging from the left upper corner (**f**, **g**) (**a** Diff-Quik, high magnification; **b**, **e** Papanicolaou stain, medium magnification; **c** MGG stain, medium magnification; **d** Diff-Quik stain, high magnification)

Metastasis from Merkel cell and small cell carcinoma should also be considered in the diagnosis.

US features. Small tumors are encapsulated, well defined, and hypoechoic. Large tumors are often infiltrative, hypoechoic, and heterogeneous with a complex echotexture reflecting areas of necrosis and hemorrhage (Fig. 5.24f, g).

Pattern VII: Large Epithelial Cell Pattern

These neoplasms can be arbitrarily divided into low-grade and high-grade types. The large cell low-grade tumors include acinic cell carcinoma, mammary analogue secretory carcinoma, oncocytic neoplasms, epithelial–myoepithelial carcinoma, clear cell adenocarcinoma, and metastasis. Those with a high-grade pattern include high-grade mucoepidermoid carcinoma, high-grade carcinoma NOS, squamous carcinoma, salivary duct carcinoma, and metastasis including, but not limited to, melanoma.

Acinic Cell Carcinoma

This is a malignant salivary gland neoplasm showing differentiation from intercalated duct/serous acinar cells. It contains cytoplasmic zymogen granules and forms various histologic patterns. Complete surgical excision is the treatment of choice; however, there is 35 % recurrence rate and 15 % metastatic rate.

Clinical findings. Acinic cell carcinoma represents approximately 20 % of salivary gland malignancies, often arises in the parotid gland, and is slightly more common in women, with a peak incidence in the seventh decade of life, but may occur at all ages, including in children, in whom it is the second frequent malignancy after mucoepidermoid carcinoma. Patients have a slow-growing mass that may be present for months or even years and are commonly asymptomatic, although some may cause vague and intermittent pain.

Histopathology. The tumor cells grow forming solid, microcystic, papillary–cystic, and follicular patterns, the first two being the most common. Papillary projections supported by

thin fibrovascular cores are present in the papillary–cystic pattern. The tumor is similar to thyroid parenchyma in the follicular-patterned tumor and has eosinophilic proteinaceous material lined by columnar or cuboidal cells.

The cellular elements may have variable proportions of *acinar cells* with polyhedral shape, eccentric round nuclei, and granular cytoplasm with zymogen granules that are characteristic of this tumor and are predominant in well-differentiated tumors. The granules are identified by electron microscopy as round electron-dense cytoplasmic secretory granules. Variable numbers of *intercalated ductal cells* with columnar or cuboidal shape, eosinophilic cytoplasm, and central nuclei, *clear cells*, and *vacuolated cells* may also be present. In summary, this tumor show different architectural patterns and cytologic findings within the same tumor. Chronic inflammation and hemorrhage may be seen. Cell pleomorphism and mitoses are usually absent.

Immunoprofile. Immunostains are not specific and show keratin positivity. Calponin, actin, and p63 are negative, with high expression for p53 and bcl-2. Acinar and intercalated cells are PAS + diastase resistant and mucicarmine negative. All other cells are PAS (-).

Molecular profile. Alterations of chromosome arms 4p, 5q, 6p, and 17p have been described.

FNA findings. Aspirates are usually cellular with cells both single and grouped, including formation of acinar arrangements (Fig. 5.25a). Thin vascular structures decorated with cellular elements of variable size and complexities are often present (Fig. 5.25b). The cytoplasmic membrane is friable, and the cells are easily damaged during the smear process, resulting in the presence of numerous naked nuclei and a granular background. Detached small fragments of vascular elements may also be found in the background. Macrophages are identified when cystic change is present.

In contrast to benign salivary gland tissue, well-differentiated acinic cell carcinoma often lacks ductal cells and adipose tissue, unless surrounding benign salivary gland tissue is inadvertently sampled. Lack of the narrow cytoplasmic rim permits the distinction of naked nuclei from small lymphocytes

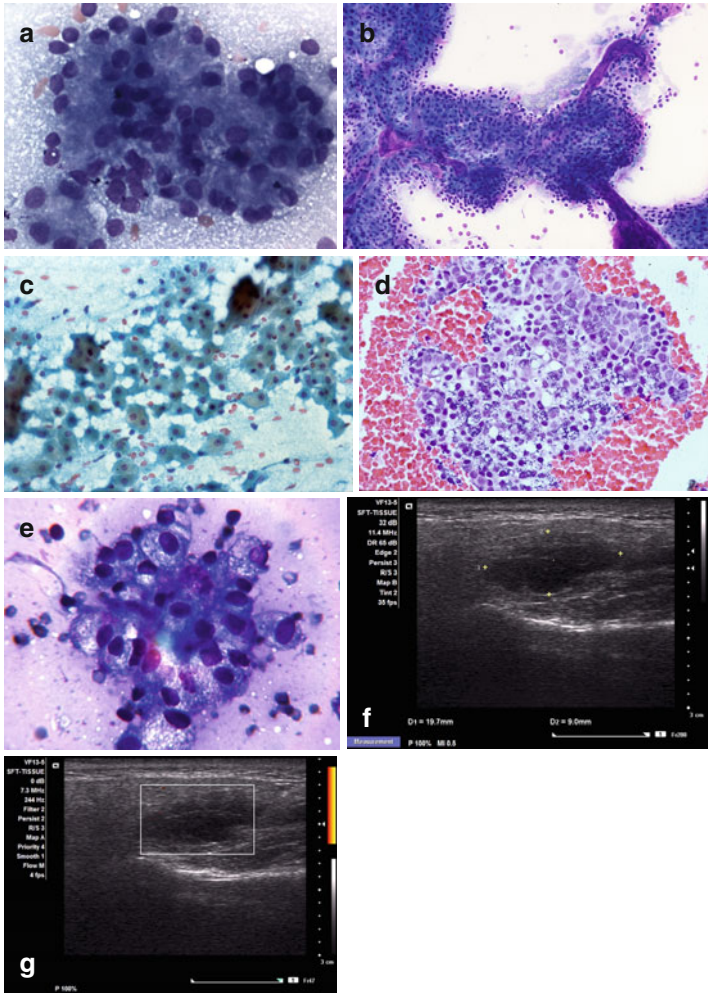

FIGURE 5.25 Acinic cell carcinoma. Cytologic features are shown in (**a**–**e**). The US images show an irregularly shaped hypoechoic mass with slight heterogeneous echotexture and no vascularity by Doppler examination (**f**, **g**) (**a**, **b**, **e** MGG stain, medium and high magnification; **c** Papanicolaou stain, medium magnification; **d** hematoxylin and eosin stain, medium magnification)

and avoids an erroneous diagnosis of Warthin's tumor, particularly in the presence of cystic change. Distinguishing oncocytoma from acinic cell carcinoma may be more challenging because the smear pattern, cellular features including nuclear characteristics, and smear background are almost identical (Fig. 5.25c). When cell block slides stained with H&E are available, the basophilic, coarse cytoplasmic granules are more conspicuous than the uniform eosinophilic granules of oncocytoma (Fig. 5.25d). Of note, clear cell change may be seen in both acinic cell carcinoma and oncocytoma, and even the possibility of epithelial–myoepithelial carcinoma, clear cell adenocarcinoma, and metastatic renal cell carcinoma may be entertained (Fig. 5.25e). Cystic acinic cell carcinoma may show vacuolated cells resembling low-grade mucoepidermoid carcinoma. Differential diagnosis includes other low-grade salivary gland neoplasms such as mucoepidermoid carcinoma and the recently described mammary analogue secretory carcinoma.

US features. The features are not specific, and the tumor is hypoechoic and heterogeneous, with areas of cystic degeneration (Fig. 5.25f, g).

Mammary Analogue Secretory Carcinoma

This tumor was described in 2010 and is strikingly similar to the secretory breast carcinoma not only morphologically but also at the molecular level with identical translocation.

Clinical findings. The tumor appears to be more common in men than in women with an average age of presentation of 45 years and predominantly affects major salivary glands. The tumor is considered of low grade, has a disease-free survival of 90 months, and may involve regional neck lymph nodes.

Histopathology. The architectural pattern is often microcystic; however, macrocystic and solid patterns have been described. Cytologically, the tumor often shows monomorphic large cells with finely vacuolated cytoplasm with bland-appearing round nuclei and small nucleoli. Few mitoses may

be present. Hobnailing, eosinophilic vacuolated cytoplasm, and variable mucin production have been described. This tumor must be distinguished from oncocytic tumors, acinic cell carcinoma, low-grade mucoepidermoid carcinoma, and salivary gland duct adenocarcinoma. The histo- and cytomorphology may be similar, and the final diagnosis rests upon the molecular detection of the specific and unique translocation.

Immunoprofile. The tumor is strongly positive for S-100 protein and mammaglobin. High-molecular-weight keratin, vimentin, and cytokeratin 19 are also positive.

Molecular profile. The translocation between the *ETV6* gene and the *NTRK3* gene located on chromosomes 12p13 and 15q25 is seen in almost 100 % of tumors and can be detected by FISH analysis in paraffin-embedded tissue or FNA cytology material.

FNA findings. Smears are cellular showing cell aggregates and single cells. Cell aggregates may have acinar, tight, small, tubular, or arborizing papillary patterns with transgressing capillaries. Cells have abundant finely granular and variably vacuolated cytoplasm, eccentrically placed round nuclei, and nucleoli of variable size. Ample eosinophilic cytoplasm, binucleation, signet ring cell-like cells, and mild to moderate nuclear atypia may be seen. Amorphous aggregates of mucin and stripped tumor cell nuclei may be seen in the background (Fig. 5.26).

Oncocytoma

This rare benign tumor that comprises <1 % of salivary gland neoplasms is composed of large cells with granular mitochondria-rich eosinophilic cytoplasm. Complete surgical excision is the treatment of choice.

Clinical findings. The tumor often occurs in the parotid gland, has no gender preference, and occurs in the sixth to eighth decade of life. Patients have a painless mass and are asymptomatic.

Histopathology. The tumor is encapsulated with a solid, organoid, and trabecular pattern composed of enlarged, polyhedral oncocytic cells with central round nuclei and conspicuous nucleoli. Cellular pleomorphism, necrosis, or mitoses

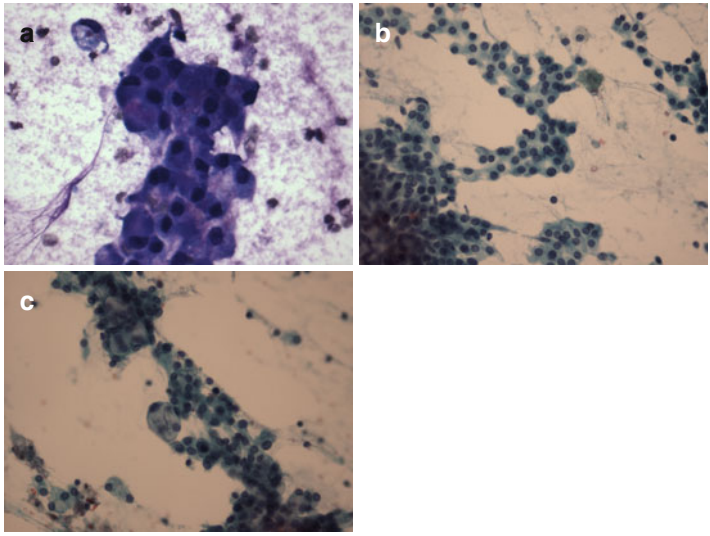

FIGURE 5.26 Mammary analogue secretory carcinoma. Smears are cellular and show cells with ample eosinophilic dense cytoplasm, granular background, and scattered stripped nuclei; large cytoplasmic vacuoles displacing the nucleus to the periphery ("signet ring-like" cells) are also noted (**a**). Papanicolaou-stained smears show sheets of large cells with eosinophilic cytoplasm, round central and eccentrically placed nuclei, and small inconspicuous nucleoli (**b**). Occasional cells with variable cytoplasmic vacuolization are also seen (**c**). Note the striking similarity with oncocytic neoplasms and acinic cell carcinoma (**a** Diff-Quik stain, high magnification; **b**, **c** Papanicolaou stain, high magnification. Courtesy, Dr. Edward B. Stelow, University of Virginia, Charlottesville, VA)

are absent. A clear cell variant, in part due to accumulation of cytoplasmic glycogen, with variable transitional cell areas may occur.

Immunoprofile. The epithelial elements show an immunoprofile similar to that of Warthin's tumor.

Molecular profile. Alterations in mitochondrial DNA mutations have not been consistently found.

FNA findings. The oncocytic cells are arranged in flat sheets, papillary clusters, and as individual cells (Fig. 5.27a–c). Cytologic atypia is focal or absent, and scattered lymphoid

cells may be present (Fig. 5.27d). Cystic changes may occur. The differential diagnosis includes oncocytosis or adenomatous hyperplasia, Warthin's tumor, pleomorphic adenoma, and salivary gland carcinoma with oncocytic cells such as mucoepidermoid carcinoma, acinic cell carcinoma, adenoid cystic carcinoma, or oncocytic carcinoma. When clear cells predominate, one should consider clear variants of epithelial–myoepithelial carcinoma, primary salivary gland adenocarcinoma, myoepithelioma, mucoepidermoid carcinoma, and metastatic renal cell carcinoma.

US features. There is no typical US pattern; this is similar to other benign lesions. The tumor is a round or oval, well-defined hypoechoic homogeneous mass. Power Doppler demonstrates peripheral and intratumor blood flow (Fig. 5.27e–h). Cystic and hemorrhagic degeneration may be seen in tumors >3 cm.

Epithelial–Myoepithelial Carcinoma

This rare, low-grade malignant neoplasm is composed of epithelial and myoepithelial cells. Complete surgical excision is the treatment of choice; however, there is a 30–50% recurrence rate and 20 % metastatic rate.

Clinical findings. The tumor often develops in the parotid gland, is slightly more common in women, and occurs in the sixth and seventh decade of life. Patients have a slow-growing, often painless mass. Facial nerve paralysis is infrequent.

Histopathology. Tumor cells often show tubular, cystic, solid, papillary, and trabecular growth patterns that are present in various proportions within the tumor. The neoplastic cells are of two types: epithelial cuboidal with scant eosinophilic cytoplasm and myoepithelial polyhedral, large cells with vacuolated clear cytoplasm. Epithelial cells are inconspicuous in solid tumors, where the myoepithelial cells predominate. Of note, the epithelial cell layer is single, but the myoepithelial cells may form several layers. A dual layer of inner epithelial and outer myoepithelial lining cells is visualized in tumors that have cystic and tubular components. The separating stroma may be fibrovascular, myxoid, hyaline, or

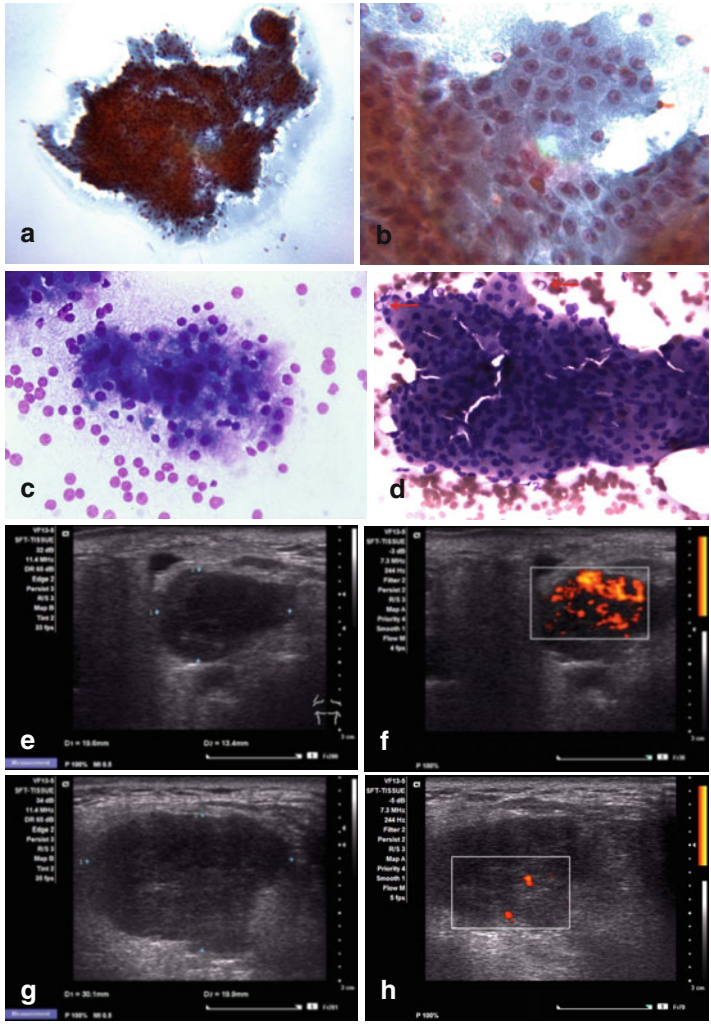

FIGURE 5.27 Oncocytoma. Cytologic features are shown in (**a**–**d**). The *red arrows* (**d**) point to rare lymphoid cells that may be found in oncocytoma. The ultrasonographic findings are not specific and are shown in (**e**–**h**) (**a**, **b** Papanicolaou stain, low and medium magnifications; **c** Diff-Quik stain, high magnification; **d** MGG stain, high magnification)

dense and is PAS positive. Mitoses, necrosis, or marked cellular anaplasia are not typically present. Oncocytic and sebaceous differentiation may occur.

Immunoprofile. The epithelial cells are positive for cytokeratin and EMA. Myoepithelial cells are p63, calponin, actin, and S-100 protein positive. Bcl-2 and c-kit are frequently positive.

Molecular profile. These tumors are reported to be aneuploid. The most frequent recurrent aberrations reported are gains of 8q (26 %) and gains of 1q (21 %) and chromosome 5 (21 %). Several oncogene candidates, including cyclin-dependent kinase 4 (*CDK4*), sarcoma-amplified sequence (*SAS*, aka tetraspanin 31 – *TSPAN31*), and glioma-associated oncogene homolog (*GLI1*), have been suggested.

FNA findings. Smears are usually cellular and show two patterns, small dark epithelial cells with scant dense cytoplasm and large myoepithelial cells with distinct borders and ample and clear cytoplasm. However, myoepithelial cells have a fragile cytoplasm and may be present as naked nuclei or cells without much cytoplasm. This may be the predominant pattern. Fragments of acellular hyaline material, which may be globular, may be present, suggesting adenoid cystic carcinoma. When clear cells predominate, alternate diagnoses to consider include clear cell adenocarcinoma, clear cell acinic cell carcinoma, or sebaceous carcinoma; however, these tumors do not exhibit a dual cell population. Thus, a thorough sampling is required for a correct diagnosis.

US features. Features of epithelial–myoepithelial carcinoma mimic those of a benign salivary gland tumor.

Clear Cell Adenocarcinoma

This is a rare malignant epithelial neoplasm composed of monotonous clear cells. The tumor has ductal but not myoepithelial cell differentiation. Complete surgical resection is the

treatment of choice for this low-grade neoplasm and the prognosis is excellent.

Clinical findings. The tumor often develops in the intraoral minor salivary glands and occurs mostly in females. There is no age preference. Patients present with swelling and may have pain and mucosal ulceration. Prognosis is good; however, local recurrence and lymph node metastases may be seen.

Histopathology. Polygonal to round cells with clear glycogen-rich cytoplasm, eccentric round nuclei, and small nucleoli are arranged in sheets, nests, and cords. Ductal structures are absent. There is mild to moderate nuclear pleomorphism, and mitoses are rare. The stroma is usually thin and fibrous, but may be broad and thick and hyalinized or loose. The differential diagnosis includes clear cell mucoepidermoid carcinoma, myoepithelial neoplasms, and metastatic renal cell carcinoma.

Immunoprofile. Tumors are strongly positive for p63, CEA, and EMA. Cytokeratin is positive. There is variable positivity with vimentin and GFAP. However, myoepithelial markers such as S-100 protein, calponin, and smooth muscle actin are usually negative.

Molecular profile. Tumors show a consistent translocation t(12;22) involving the *EWSR1* (Ewing sarcoma breakpoint region *1*) gene and the *ATF1* gene. This marker may be used to differentiate this tumor from other salivary gland tumors that do not harbor this translocation such as myoepithelioma, acinic cell carcinoma, pleomorphic adenoma, mucoepidermoid carcinoma, oncocytic neoplasms, salivary duct carcinoma, adenoid cystic carcinoma, and pleomorphic low-grade adenocarcinoma.

FNA findings. Smears are cellular and show groups and sheets of cells with well-defined cytoplasmic borders, uniform round nuclei, small nucleoli, and abundant clear cytoplasm. Hyaline globules are absent, although fragments of hyalinized stroma may be present.

Salivary Duct Carcinoma

This high-grade malignancy arises from the excretory ducts and resembles breast carcinoma on histology. Treatment of choice includes complete excision with radical neck dissection and postoperative radiotherapy. There is a 30–40 % recurrence rate, 50–60 % metastatic rate, and 60–80 % mortality rate.

Clinical findings. This rare tumor is more common in men, often occurs after the age of 50 years, and commonly affects the parotid gland. When the parotid gland is affected, patients have a rapidly growing mass, with or without local pain and/or facial nerve paralysis.

Histopathology. The tumor resembles the pathologic findings of intraductal and infiltrating ductal breast carcinoma, including comedo necrosis and cribriform, solid, cystic, and papillary patterns. Neoplastic cells are large with large hyperchromatic nuclei, prominent nucleoli, and slightly eosinophilic cytoplasm. Necrosis and mitosis are often present. Squamous metaplasia, oncocytic changes, chronic inflammation, and psammoma-like bodies may be present. Histologic variants including sarcomatoid, micropapillary, mucin-rich, and osteoclast-like giant cell may occur, as in breast carcinoma

Immunoprofile. Salivary duct carcinoma expresses some markers also found in breast carcinoma. Gross cystic disease fluid protein-15 (GCDFP-15) is found in 80 % of cases. HER2/neu is positive in 90 % of cases; however, it depends on the antibody clone used and scoring system. Cytokeratin, EMA, and CEA are also positive. ER and PR expression is exceptional; in contrast, androgen receptor (AR) positivity is seen in 67–83 % of cases. Myoepithelial differentiation markers including p63, calponin, smooth muscle actin, and vimentin are negative. Following the breast cancer molecular classification, attempt to classify 42 pure salivary duct carcinomas into molecular subtypes showed that 16.7, 69, 4.8, 9.5, and 0 % were of HER2, luminal AR-positive, basal-like,

indeterminate, and luminal phenotype, respectively. The prognostic implications of this classification and possible targeted therapy for these tumors need to be evaluated.

Molecular profile. There is loss of heterozygosity of polymorphic markers of chromosome locus 9p21 containing the tumor suppressor gene *p16*(INK4a/CDKN2/MTS1). The apoptosis-related genes *CASP10* and *MMP11* are overexpressed.

FNA findings. Smears are cellular and show complex tridimensional aggregates. Flat sheets are present arranged in cribriform, solid, and papillary patterns. Occasional psammoma bodies, squamous metaplastic cells, and comedo-like necrosis may be seen. Cells are large and polyhedral with granular or vacuolated cytoplasm, large hyperchromatic nuclei, prominent nucleoli, and increased mitotic activity (Fig. 5.28).

US features. In one reported case of salivary duct carcinoma of the extra-glandular segment of Stensen's duct, the scan showed an ill-defined hypoechoic tumor and a dilated and thickened wall of the duct connected with the tumor.

Malignant neoplasms showing large cells and a high nuclear grade, including metastases, are rare, and a specific FNA diagnosis cannot be made in most cases. It is sufficient to state the diagnosis of a high-grade malignancy and exclude direct extension of a head and neck tumor or metastasis to the salivary gland or intraparotid lymph node to avoid unnecessary surgery. A clinical history of previous malignancy is of extreme importance. In general, a metastatic deposit must be suggested when the smear pattern is different from that of known salivary gland malignancies (Fig. 5.29).

Pattern VIII: Spindle Cell Pattern

Processes showing this pattern can be divided into low grade and high grade. Myoepithelioma is the typical example of low-nuclear-grade lesions, and primary or secondary sarcomas, malignant myoepithelioma, and malignancies with

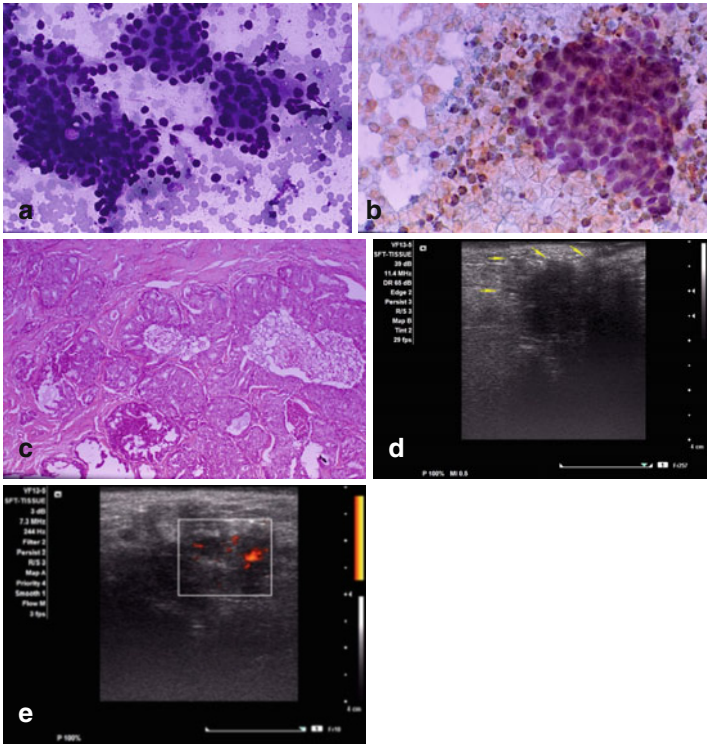

FIGURE 5.28 Salivary duct carcinoma. Cytologically and histologically, this tumor is almost indistinguishable from ductal breast carcinoma. Ultrasound imaging from a different case shows a heterogeneous mass with spiculated fuzzy borders (**d**, *arrows*) and irregular vascular flow by Doppler examination (**e**) (**a** Diff-Quik stain, medium power; **b** Papanicolaou stain, medium power; **c** hematoxylin and eosin stain, medial magnification)

spindle cell morphology including metastatic melanoma should be considered in the high-grade group. These tumors are rarely described in either the histopathology or cytology literature.

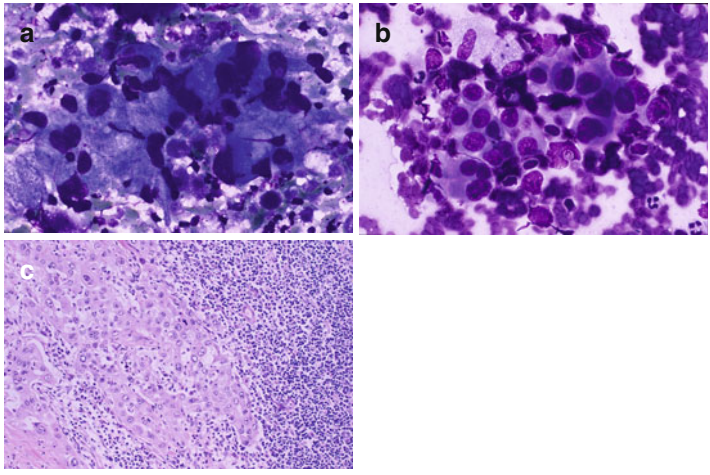

FIGURE 5.29 Metastatic adenocarcinoma from pulmonary origin (**a**). Metastatic squamous cell carcinoma to an intraparotid lymph node (**b**) with histologic correlation (**c**) (**a**, **b** Diff-Quik stain, high magnification; **c** hematoxylin and eosin stain, medial magnification)

Myoepithelioma

This tumor is a benign neoplasm composed of spindle, epithelioid, plasmacytoid, or clear cells. Complete surgical excision is the treatment of choice. Recurrence is related to incomplete excision.

Clinical findings. This slow-growing tumor is rare, has no gender predilection, often occurs in adults with an average age of 44 years, and develops preferentially in the parotid gland.

Histopathology. Spindle cells are arranged in interlacing fascicles resembling stroma. Plasmacytoid cells are often seen in myoepitheliomas arising in the minor salivary glands. The stroma is collagenous or mucoid.

Immunoprofile. Cells are positive for cytokeratins. Spindle cells show variable reactivity with actin, calponin, S-100 protein, GFAP, and smooth muscle myosin heavy chain.

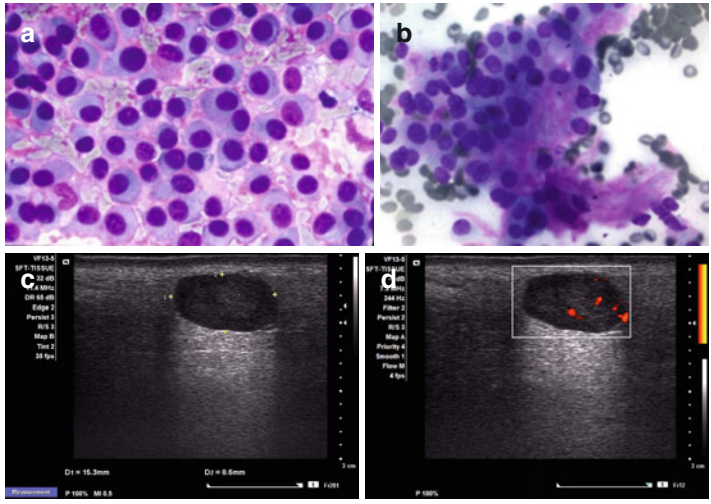

Figure 5.30 Myoepithelioma. Numerous myoepithelial cells are present both single and supported by a collagenous stroma with lack of fibrillary magenta features (**a**, **b**). The US findings are non-specific including oval, slightly lobulated well-defined tumor edges, marked hypoechogenicity, and minimal internal vascularity by Doppler examination (**c**, **d**) (**a** Diff-Quik stain; **b** MGG stain, high magnification)

Molecular profile. Alterations of chromosomes 1, 9, 12, and 13 have been detected.

FNA findings. Smears are cellular and show bland-appearing, uniform spindle, epithelioid/plasmacytoid, and stellate cells. Nuclear grooves and intranuclear inclusions may be present. Scant myxoid and fibrillary matrix may be seen and in some cases may have a globular appearance resembling adenoid cystic carcinoma (Fig. 5.30a, b).

US features. The sonographic characteristics of benign and malignant neoplasms have no significant differences. Thus, US cannot differentiate with certainty between benign and malignant cases, particularly in low-grade neoplasms

(Fig. 5.30c, d). US findings reported in a 7.8-cm tumor included a well-circumscribed mass with solid and cystic components and posterior acoustic enhancement.

Myoepithelial Carcinoma

This tumor is the malignant counterpart of myoepithelioma.

Clinical findings. This tumor is rare, has no gender predilection, occurs in adults, and commonly affects the parotid gland. Patients often have a slow-growing, asymptomatic mass.

Histopathology. Various proportions of spindle, plasmacytoid, epithelioid, and clear cells with variable nuclear pleomorphism are seen. Variable amounts of myxoid or mucoid stroma may be seen and, in some areas, may appear globular and eosinophilic. Cystic changes may be present. In the absence of malignant cytomorphology, invasion into surrounding tissue is the only indication of malignancy.

Immunoprofile. Cytokeratin is positive, as are myoepithelial markers such as calponin, p63, actin, S-100 protein, and vimentin.

Molecular profile. Infrequent cytogenetic alterations have been seen.

FNA findings. The findings are similar to those of myoepithelioma; however, marked nuclear pleomorphism, atypical mitosis, and necrosis may be present (Fig. 5.31a–c).

US features. One reported case describes a hypoechogenic and heterogeneous 2-cm tumor with irregular borders, invading the surrounding soft tissue including the masseter muscle and subcutaneous tissue; Doppler examination showed a hilar vascular pattern (Fig. 5.31d, e).

In summary, USG-FNA should be considered in the diagnostic evaluation of a patient with a salivary gland mass, allowing for optimal surgical planning and preoperative patient counseling. It has >90 % sensitivity and specificity, modifies or avoids surgery in 30 % of cases, and procures material for ancillary tests, including molecular studies potentially useful for targeted therapy.

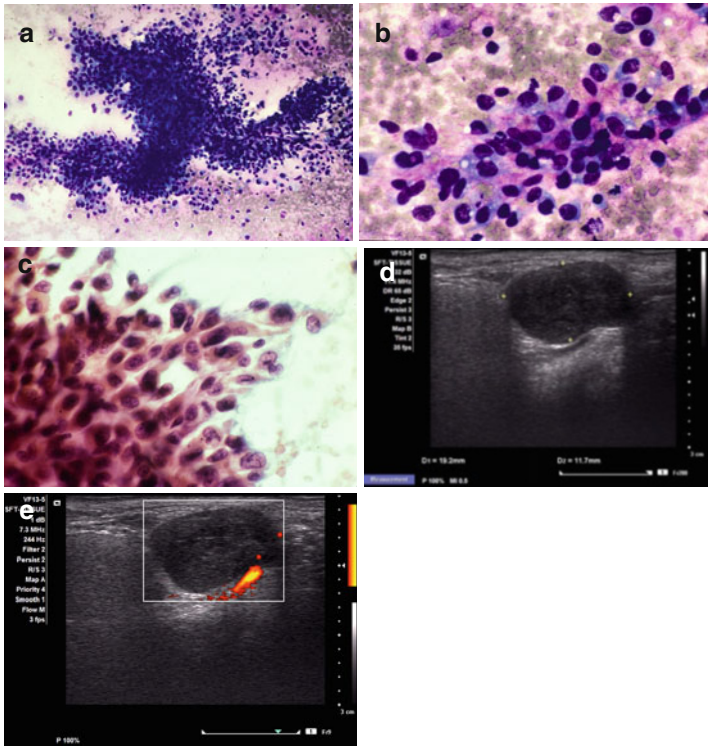

FIGURE 5.31 Malignant myoepithelioma. Smears show high cellularity, branching complex pseudopapillary aggregates, plasmacytoid and spindle cell features, and nuclear atypia (**a**–**c**). Ultrasound imaging shows a well-circumscribed homogeneous hypoechoic mass with posterior acoustic enhancement and minimal vascularity by Doppler examination (**d**–**e**) (**a**, **b** MGG stain, medium and high magnification; **c** Papanicolaou stain, high magnification)

Suggested Reading

Barnes L, Eveson JW, et al. Salivary glands. In: Barnes L, Eveson JW, Reichart P, Sidransky D, editors. Pathology and genetics of head and neck tumors. Lyon: IARC; 2005. p. 209–81.

Brill 2nd LB, Kanner WA, et al. Analysis of MYB expression and MYB-NFIB gene fusions in adenoid cystic carcinoma and other salivary neoplasms. Mod Pathol. 2011;24(9):1169–76.

Di Palma S, Simpson RH, et al. Salivary duct carcinomas can be classified into luminal androgen receptor-positive, HER2 and basal-like phenotypes*. Histopathology. 2012;61(4):629–43.

El-Naggar AK. Celular and molecular pathology of head and neck tumors. In: Bernier J, editor. Head and neck cancer: multimodality management. New York: Springer; 2011. p. 57–79.

Geisinger KR, Stanley MW, et al. Salivary gland masses. In: Modern cytopathology. Philadelphia: Churchill Livingstone; 2004. p. 781–811.

Griffith CC, Stelow EB, et al. The cytological features of mammary analogue secretory carcinoma: a series of 6 molecularly confirmed cases. Cancer Cytopathol. 2013;121(5):234–41.

Gupta S, Sodhani P, et al. Oncocytic papillary cystadenoma of parotid gland: a diagnostic challenge on fine-needle aspiration cytology. Diagn Cytopathol. 2011;39(8):627–30.

Henry-Stanley MJ, Beneke J, et al. Fine-needle aspiration of normal tissue from enlarged salivary glands: sialosis or missed target? Diagn Cytopathol. 1995;13(4):300–3.

Johnson FB, Oertel YC, et al. Sialadenitis with crystalloid formation: a report of six cases diagnosed by fine-needle aspiration. Diagn Cytopathol. 1995;12(1):76–80.

Kim J, Kim EK, et al. Characteristic sonographic findings of Warthin's tumor in the parotid gland. J Clin Ultrasound. 2004;32(2):78–81.

Klijanienko J, el-Naggar AK, et al. Comparative cytologic and histologic study of fifteen salivary basal-cell tumors: differential diagnostic considerations. Diagn Cytopathol. 1999a;21(1):30–4.

Klijanienko J, El-Naggar AK, et al. Fine-needle sampling findings in 26 carcinoma ex pleomorphic adenomas: diagnostic pitfalls and clinical considerations. Diagn Cytopathol. 1999b;21(3):163–6.

Klijanienko J, Lagace R, et al. Fine-needle sampling of primary neuroendocrine carcinomas of salivary glands: cytohistological correlations and clinical analysis. Diagn Cytopathol. 2001;24(3):163–6.

Klijanienko J, Vielh P. Fine-needle sampling of salivary gland lesions. I. Cytology and histology correlation of 412 cases of pleomorphic adenoma. Diagn Cytopathol. 1996;14(3):195–200.

Klijanienko J, Vielh P. Fine-needle sample of salivary gland lesions. V: Cytology of 22 cases of acinic cell carcinoma with histologic correlation. Diagn Cytopathol. 1997a;17(5):347–52.

Klijanienko J, Vielh P. Fine-needle sampling of salivary gland lesions. II. Cytology and histology correlation of 71 cases of Warthin's tumor (adenolymphoma). Diagn Cytopathol. 1997b;16(3):221–5.

Klijanienko J, Vielh P. Fine-needle sampling of salivary gland lesions. III. Cytologic and histologic correlation of 75 cases of adenoid

cystic carcinoma: review and experience at the Institut Curie with emphasis on cytologic pitfalls. Diagn Cytopathol. 1997c;17(1):36–41.
Klijanienko J, Vielh P. Fine-needle sampling of salivary gland lesions. IV. Review of 50 cases of mucoepidermoid carcinoma with histologic correlation. Diagn Cytopathol. 1997d;17(2):92–8.
Klijanienko J, Vielh P. Cytologic characteristics and histomorphologic correlations of 21 salivary duct carcinomas. Diagn Cytopathol. 1998a;19(5):333–7.
Klijanienko J, Vielh P. Fine-needle sampling of salivary gland lesions. VI. Cytological review of 44 cases of primary salivary squamous-cell carcinoma with histological correlation. Diagn Cytopathol. 1998b;18(3):174–8.
Klijanienko J, Vielh P. Fine-needle sampling of salivary gland lesions. VII. Cytology and histology correlation of five cases of epithelial-myoepithelial carcinoma. Diagn Cytopathol. 1998c;19(6):405–9.
Klijanienko J, Vielh P. Salivary carcinomas with papillae: cytology and histology analysis of polymorphous low-grade adenocarcinoma and papillary cystadenocarcinoma. Diagn Cytopathol. 1998d;19(4):244–9.
Lee YYP, Wong KT, et al. Ultrasound investigations in head and neck cancer patients. In: Bernier J, editor. Head and neck cancer: multimodality management. New York: Springer; 2011. p. 221–33.
Mukunyadzi P. Review of fine-needle aspiration cytology of salivary gland neoplasms, with emphasis on differential diagnosis. Am J Clin Pathol. 2002;118(Suppl):S100–15.
Okada F, Honda K, et al. Salivary duct carcinoma of the extra-glandular segment of Stensen's duct: radiological findings and pathological correlation (2008: 10b). Eur Radiol. 2009;19(1):254–7.
Rhys R. Ultrasound of the neck. In: Allan PL, Baxter GM, Weston MJ, editors. Clinical ultrasound, vol. 2. London: Churchill Livingstone Elsevier; 2011. p. 890–919.
Rosai J. Major and minor salivary glands. In: Rosai J, editor. Rosai and Ackerman's surgical pathology, vol. 1. Edinburgh: Mosby Elsevier; 2011. p. 817–56.
Shah AA, LeGallo RD, et al. EWSR1 genetic rearrangements in salivary gland tumors: a specific and very common feature of hyalinizing clear cell carcinoma. Am J Surg Pathol. 2013;37(4):571–8.
Shi L, Wang YX, et al. CT and ultrasound features of basal cell adenoma of the parotid gland: a report of 22 cases with pathologic correlation. AJNR Am J Neuroradiol. 2012;33(3):434–8.
Skalova A, Vanecek T, et al. Mammary analogue secretory carcinoma of salivary glands, containing the ETV6-NTRK3 fusion

gene: a hitherto undescribed salivary gland tumor entity. Am J Surg Pathol. 2010;34(5):599–608.
Stanley MW. Selected problems in fine needle aspiration of head and neck masses. Mod Pathol. 2002;15(3):342–50.
Stanley MW, Bardales RH, et al. Sialolithiasis. Differential diagnostic problems in fine-needle aspiration cytology. Am J Clin Pathol. 1996a;106(2):229–33.
Stanley MW, Bardales RH, et al. Primary and metastatic high-grade carcinomas of the salivary glands: a cytologic-histologic correlation study of twenty cases. Diagn Cytopathol. 1995;13(1):37–43.
Stanley MW, Horwitz CA, et al. Basal cell carcinoma metastatic to the salivary glands: differential diagnosis in fine-needle aspiration cytology. Diagn Cytopathol. 1997;16(3):247–52.
Stanley MW, Horwitz CA, et al. Basal-cell adenoma of the salivary gland: a benign adenoma that cytologically mimics adenoid cystic carcinoma. Diagn Cytopathol. 1988;4(4):342–6.
Stanley MW, Horwitz CA, et al. Basal cell (monomorphic) and minimally pleomorphic adenomas of the salivary glands. Distinction from the solid (anaplastic) type of adenoid cystic carcinoma in fine-needle aspiration. Am J Clin Pathol. 1996b;106(1):35–41.
Tsuneki M, Maruyama S, et al. Podoplanin is a novel myoepithelial cell marker in pleomorphic adenoma and other salivary gland tumors with myoepithelial differentiation. Virchows Arch. 2013;462(3):297–305.
Wenig BM. Major and minor salivary glands. In: Atlas of head and neck pathology. Philadelphia: Saunders Elsevier; 2008. p. 536–702.
Yuan WH, Hsu HC, et al. Gray-scale and color Doppler ultrasonographic features of pleomorphic adenoma and Warthin's tumor in major salivary glands. Clin Imaging. 2009;33(5):348–53.
Zhang C, Cohen JM, et al. Fine-needle aspiration of secondary neoplasms involving the salivary glands. A report of 36 cases. Am J Clin Pathol. 2000;113(1):21–8.